High Resolution Geophysical Characterization of a Gasoline Release into a Sand Column

by

Fatemeh Vakili

A thesis
presented to the University of Waterloo
in fulfillment of the
thesis requirement for the degree of
Master of Science
in
Earth Sciences

Waterloo, Ontario, Canada, 2008

AUTHOR'S DECLARATION

I hereby declare that I am the sole author of this thesis. This is a true copy of the thesis, including any required final revisions, as accepted by my examiners.

I understand that my thesis may be made electronically available to the public.

Abstract

A controlled column experiment was conducted to investigate the geophysical response of gasoline spills into the partially saturated sand column. The column was 0.61 diameter (ID) and 2 m high cylindrical polyvinyl chloride, which was packed with the Borden sand to a height of 1.95 m, flushed with CO_2, saturated, and drained to a height of 0.73 m. The monitoring techniques used for this experiment was DC resistivity and time domain reflectometry (TDR) methods. The column was equipped with resistivity electrodes and TDR probes, which were placed on the column wall vertically with 3 cm intervals, on opposite sides, two monitoring wells, an injection well, a manometer, an outlet/inlet system, and a vent. A total amount of 5 liters of standard API 91-01 gasoline was added to the system in steps of 1, 2, and 2 liters to examine the geophysical response to different amounts of gasoline.

Measurements were taken before and after each injection and also during subsequent fluctuation of the water table. Both monitoring techniques were able to record even the minor changes in the trend of conductivity and permittivity profiles due to the addition of the small amount of gasoline during the first spill. The conductivity and permittivity profiles obtained before lowering the water level below the original level and those obtained after the water level reached to the original level do not match, which is an indication of entrapped gasoline inside the pores. Two core samples was taken from the sand symmetrically after each water table fluctuation and analyzed for total petroleum hydrocarbon (TPH) analysis and the results were compared to the conductivity and permittivity results.

The conductivity profile obtained using DC resistivity method was compared to that of obtained using TDR method. The profiles match in the saturated zone where all of the pores are connected with water and therefore electrolytic conduction is predominant. In the unsaturated zone, where there is low pore water connectivity, TDR measured conductivity values are higher than those measured using the resistivity method.

Water saturation values were calculated using conductivity and permittivity values before and after each injection. Different values of saturation exponent (n) were tested for Archie's law until an appropriate value was found which gave the best water saturation from conductivity data for clean Borden sand. Then, the water saturation obtained from permittivity values using Topp's equations for different materials were compared to that of obtained from conductivity values using Archie's

equation. Topp's equation for 30 μm glass beads provided the best match. Furthermore, other equations developed by other researchers were examined to obtain water saturation profiles from the permittivity values; all of them overestimate the water saturation for Borden sand. The water saturation profiles after the gasoline spills obtained using both Archie's law and Topp's equation do not match, perhaps because both equations were developed for three-phase (water-solid-air) systems.

Acknowledgements

My special thanks go to my supervisors, Dr. Jim Barker and Dr. Tony Endres for their help, guidance, and support over the course of my graduate studies. I would also like to thank the members of my committee Dr. Jim Smith and Dr. Neil Thomson for thorough review of the work.

Thanks to Andy Colclough in the Science Machine Shop who built my experimental column, and Bob Ingleton and Paul Johnson for the technical support and permitting to access their laboratory facilities. I appreciate Leif Nelson's assistance in collecting Borden sand for the column.

I am grateful to Dr. Edwin Cey, Juliana Freitas, and Scott Piggott for their valuable suggestions and guidance throughout my experiment.

I would like to thank Marianne VanderGriendt and Shirley Chatten in the Organic Geochemistry Lab for the laboratory analysis support.

Finally, I would like to thank my family and friends, especially my husband Reza and my parents, for their support and encouragement throughout my education.

Table of Contents

List of Figures

List of Tables

Chapter 1

Introduction

Light non-aqueous phase liquids (LNAPLs1) such as gasoline and diesel fuel are common sources of groundwater contamination worldwide. They can contaminate the subsurface by spill or leakage during transport or storage in the underground storage tanks.

Knowledge of the extent of a contaminant plume is necessary for remediation the contaminated site. There are several nondestructive and destructive methods that are currently used for detecting LNAPLs in the subsurface. Geophysical methods such as time domain reflectometry (TDR), direct current (DC) electrical resistivity, neutron probe, ground penetrating radar (GPR), electromagnetic induction (EMI) are nondestructive and relatively fast. Geophysical techniques have been used widely for detecting LNAPLs and measuring fluid content of a medium (Olhoeft, 1992; DeRyck, 1994; Redman et al. 1994; Persson and Berndtsson, 2002; Haridy et al., 2004). Destructive methods deal with taking the soil samples from the subsurface and chemically analyzing them in the laboratory.

In this experiment, TDR and DC resistivity methods were used to examine the geophysical response of the partially-saturated Borden sand to the injection of different amount of gasoline and to fluctuation of the water table after the sand was contaminated. TDR is a nondestructive fast method that measures the dielectric permittivity and conductivity of a medium at the same time. Dielectric permittivity is a measure of the ability of a material to be polarized by an electric field. Since the dielectric permittivity of water (~80) is much higher than that of air (1), soil (~4), and gasoline (3-5), dielectric permittivity of a medium is dominant by its water content. Several researchers have done calibration of time domain reflectometry on different materials to find the corresponding volumetric water content from the measured dielectric permittivity and came up with different equations (Birchak et al., 1976; Topp et al., 1980; Ledieu et al., 1986; Roth et al., 1990; Jacobsen and Schjønning, 1993; Heimovaara, 1993; Ferré et al., 1996).

Persson and Berndtsson (2002) and Haridy et al. (2004) put an effort into finding the volumetric NAPL content of a four-phase system (sand-water- air-NAPL) using TDR measured dielectric permittivity and electrical conductivity. Redman and DeRyck (1994) used a combination of data from TDR and neutron probe methods to determine the volumetric LNAPL content.

To better understand how the electrical conductivity and dielectric permittivity of Borden sand change due to a gasoline spill and water table fluctuation, a column experiment was conducted in summer and fall of 2007. The column was designed to be tall (2 m) so we could have a full-saturation zone, a transition zone, and a residual-saturation zone like natural cases. The diameter of the column was big enough (0.61) so that the two monitoring technique did not affect each other. The small (0.03 m) interval between TDR probes and between resistivity electrodes helped in collecting high resolution measurements, therefore recording the minor variations throughout the experiment. The concepts of the TDR and resistivity methods, design and packing of the column, and preliminary results before the experiment was started are found in Chapter 2. The geophysical results are discussed in Chapter 3. Water saturations calculated using different equations from conductivity and dielectric permittivity data before and after gasoline injection, and comparison of the water saturations determined using each technique are presented in Chapter 4. Conclusion and recommendation are found in Chapter 5.

Chapter 2
Methodology

In this chapter, theory and application of the monitoring techniques and design of the column will be discussed.

2.1 Geophysical Monitoring Techniques

2.1.1 Time Domain Reflectometry (TDR)

Time domain reflectometry is a nondestructive, rapid method for measuring dielectric permittivity and electrical conductivity of a medium. Fellner-Feldegg (1969) first used time domain reflectometry to measure the dielectric permittivity of materials. A TDR device includes a pulse generator that produces a fast rise voltage step. The voltage pulse propagates as an electromagnetic wave along a transmission line and continues to travel in the soil through conductors called TDR probes. When the wave reaches the beginning of the rod, some of the energy is reflected back to the instrument. At the end of the probes, any remaining energy is reflected back to the instrument. The waveform obtained from the TDR displays the voltage or reflection coefficient as a function of time (Figure 2-1). Therefore, the propagation velocity can be calculated using the length of the probes (L) and the two-way traveling time of the electromagnetic wave,

$$v = \frac{2L}{t} \qquad 2\text{-}1$$

The propagation velocity of the wave is related to the relative dielectric permittivity (κ) of the medium (Fellner-Feldegg, 1969),

$$v = \frac{c}{\sqrt{\kappa}} \qquad 2\text{-}2$$

where c is the speed of the light in the vacuum. Then the permittivity of the soil can be expressed as:

$$\kappa = \left(\frac{ct}{2L} \right)^2 \qquad 2\text{-}3$$

The dielectric permittivity of a material (κ^*) is a complex value and consists of a real part κ' and an imaginary part κ'' or the electric loss:

$$\kappa^* = \kappa^{'} + i[\kappa" + (\sigma_{dc}/\omega\varepsilon_0)] \quad 2\text{-}4$$

where i is the imaginary number $(-1)^{1/2}$, σ_{dc} is the zero-frequency conductivity, ω is the angular frequency, and ε_0 is the free space permittivity. At frequencies above 1 MHz, κ'' is much less than κ' and can be neglected. Hence, the measured dielectric permittivity is called the apparent dielectric permittivity (κ_a) (Topp et al., 1980).

Dielectric permittivity is the ability of the charges in a material to be polarized in an alternating electrical field. Water is an extremely polar molecule and has a very high dielectric constant (80) compared to that of air (1), common soil minerals (3-7), and organic materials (2-5) (Topp and Ferré, 2002). Thus, the permittivity of a soil is strongly influenced by its water content.

In the early 1970s, the correlation of dielectric permittivity with volumetric water content was investigated by Davis and Chubodiac (1975). Topp et al. (1980) performed a series of 18 experiments to quantitatively describe the dependence of dielectric permittivity on the volumetric water content. Based on these experiments, Topp also determined the influence of soil type, temperature, and salt content on the relationship between dielectric permittivity and water content; however, the results showed that the relationship is relatively independent of those parameters. The following empirical relationship between the apparent dielectric permittivity (κ_a) and water content was defined by Topp et al. (1980):

$$\kappa_a = A + B\theta + C\theta^2 - D\theta^3 \quad 2\text{-}5$$

where θ is the water content; A, B, C, and D are coefficients which vary for different materials.

Topp's equation for all mineral soil is as follows:

$$\kappa_a = 3.03 + 9.3\theta + 146\theta^2 - 76.7\theta^3 \quad 2\text{-}6$$

Since we usually measure κ_a and want to determine θ, we must find the third-order polynomial equation which assumes κ_a is known. The inverse equation Topp provided in his paper (1980) for the all mineral soils is:

$$\theta = -5.3 \times 10^{-2} + 2.92 \times 10^{-2}\kappa_a - 5.5 \times 10^{-4}\kappa_a^2 + 4.3 \times 10^{-6}\kappa_a^3 \quad 2\text{-}7$$

This relationship has been used widely to estimate the water content in different media such as Fe-rich volcanic soils (Grantz et al., 1990), oil shale waste (Reeves and Elgezawi, 1992), and gravelly

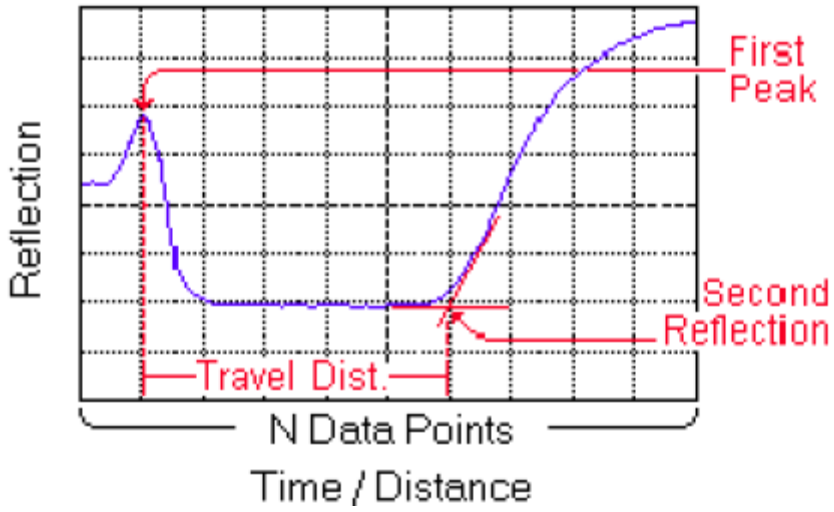

Figure 2-1 Sample TDR waveform; the pulse produced by the TDR instrument propagates through the transmission line until reaches the beginning of the rods. At this time, some of the energy reflects back to the pulse generator and the first peak appears on the oscilloscope. However, remaining energy continue to travel along the rods. After the wave reaches to the end of the rods, reflects back to the pulse generator again (second reflection). Double tangent intersecting lines show the corresponding time of the reflections.

soils (Drungil at al., 1989), as well as the unfrozen water content of frozen soils (Patterson and Smith, 1980, 1981). Patterson and Smith (1985) modified Topp's equation for frozen soils with low liquid water content. However, the results of several other studies on soils with high organic material or clay content (Dasberg and Hopmans, 1992; Roth et al., 1992, 1993, Weitz et al., 1997) were not well described by Topp's equation.

Other scientists have studied the relationship between dielectric permittivity and water saturation, and proposed calibration relationships to relate the water content to the measured apparent dielectric permittivity. For example, Jacobsen and Schjønning (1993) measured the water content of 189 soil samples, ranging from coarse sand to a sandy clay loam. Using gravimetric water content values and the apparent dielectric content obtained from TDR method, they proposed a third-order polynomial relationship between θ and κ_a:

$$\theta = -7.01 \times 10^{-2} + 3.47 \times 10^{-2}\kappa_a - 11.6 \times 10^{-4}\kappa_a^2 + 18.0 \times 10^{-6}\kappa_a^3 \quad \text{2-8}$$

Ferré et al. (1996) showed that $\kappa^{1/2}$ is a linear function of the water content θ:

$$\theta = a\kappa^{1/2} + b \quad \text{2-9}$$

where a and b are constants with values of 0.1181 and -0.1841, respectively.

In contrast to empirical relationships, dielectric mixing models relate the composite dielectric permittivity of a mixture to the dielectric permittivity and volume fraction of its constituents. Birchak et al. (1974) presented a model which is commonly used in TDR application:

$$\kappa_a^\alpha = \sum_i \theta_i \kappa_i^\alpha \quad \text{2-10}$$

where θ_i and κ_i are the volume fraction and the dielectric permittivity of component i. The term α is a parameter accounting for soil geometry; α=1 if the electric field is parallel to the layering and α=-1 if the electric field is perpendicular to the layering (Brown, 1956). Birchak et al. (1974) found α=0.5 for an isotropic two-phase medium based on the wave propagation principles. Roth et al. (1990) extended the mixing model to a three-phase system:

$$\kappa_a^\alpha = \theta\kappa_w^\alpha + (1-\phi)\kappa_s^\alpha + (\phi-\theta)\kappa_{air}^\alpha \quad \text{2-11}$$

where θ is the volumetric water content, ϕ is the porosity, κ_w, κ_s, and κ_{air} are the permittivity of water, solid, and air, respectively; α value was determined to be close to 0.5 for their study.

Persson and Berndtsson (2002) used four-phase dielectric mixing model to find κ_a:

$$\kappa_a^\alpha = \theta_w\kappa_w^\alpha + (1-\phi)\kappa_s^\alpha + (\phi-\theta_w-\theta_{NAPL})\kappa_{air}^\alpha + \theta_{NAPL}\kappa_{NAPL}^\alpha \quad \text{2-12}$$

θ_{NAPL} is the volumetric NAPL content and κ_{NAPL} is dielectric permittivity of NAPL. They performed calibration experiments on 43 samples with different combinations of θ_{NAPL} and θ_w and found that equation 2-11 overestimate the κ_a if α was kept constant. They showed that α value decreased significantly when θ_{NAPL} increased.

2.1.1.1 Application

The TDR probes used for this experiment are stainless steel welding rods that are inserted into the column through nylon Swagelok fittings. There are a total of 61 TDR rods installed from a height of 15 cm to 190 cm at 3 cm vertical intervals. Knight (1992) showed that in two-rod TDR probes, the diameter of the rods should not be less than 0.1 of the distance between them in order to avoid the

concentration of too much energy around the rods. Therefore, the rods were chosen to be 0.3 cm in diameter. The rods are 27 cm in length, of which 21.3 cm is inside the column in the soil.

In this experiment, the Tektronix 1502C (TDR Cable Tester) was used to measure the dielectric permittivity. A coaxial cable was used to connect the instrument to the rods. Two connectors were attached to one end of the cable which conducted the electromagnetic waves to two rods at the same time. Therefore, this system is similar to commercial two-rod probe with the difference being that the end of the rods was not fixed. The advantage of not having a fixed end for each probe was that water content could be measured for each interval. The total number of 61 single rods gave us the ability to perform 60 water content measurements along the column. TDR measurements were taken before and after each gasoline spill, as well as during the lowering and raising of the water level.

Volumetric water content, dielectric permittivity, and electrical conductivity of the soil was obtained using the WinTDR (version 6) program; a Windows-based program which was written by the Soil Physics Group at Utah State University. The program uses the Topp's equation for all mineral soil to calculate the water content from the measured dielectric permittivity values.

2.1.2 Direct Current (DC) Resistivity

Due to the insulating nature of soil grains, the resistivity, and its inverse conductivity ($\sigma=1/\rho$), of a clean (i.e., clay free) porous medium is dependent on the state and distribution of the electrically conductive water (i.e., aqueous phase) in the pore space. For a water saturated medium, its conductivity is a function of the pore space volume and connectivity. Since the conductivity of water is very high compared to that of air ($\sigma \approx 0$ mS/m) and other non-aqueous pore fluid phases (e.g., gasoline), the conductivity of a partial saturated medium is dependent on its water saturation and pore scale distribution of the aqueous phase.

The well-known Archie's empirical law can be used to convert the conductivity values to water saturation (Archie 1942):

$$\sigma_a = a\phi^m S_w{}^n \sigma_w \qquad 2\text{-}13$$

where σ_a is the apparent soil electrical conductivity; a is an empirical constant, usually assumed as 1; ϕ is the porosity; m is the cementation factor; n is the saturation exponent; S_w is the degree of saturation; and σ_w is the pore water conductivity. Assuming a and m are independent of σ_w and S_w, the saturation corresponding to a measured σ_a can be calculated as:

$$\frac{\sigma_a}{\sigma_{sat.}} = \frac{a\phi^m S_w{}^n \sigma_w}{a\phi^m 1^n \sigma_w} \quad 2\text{-}14$$

$$S_w = \left(\frac{\sigma_a}{\sigma_{sat.}} \right)^{\frac{1}{n}} \quad 2\text{-}15$$

For equation 2-15, prior knowledge of porosity and pore water conductivity is not required. Archie stated in his paper that this equation can be applied for the water saturations down to 0.15 or 0.2.

DC resistivity technique is an indirect method for determining the water content of a medium using resistivity values. All resistivity methods introduce an artificial source of current into the soil through the current electrodes and measure potential at the other electrodes which are placed at the vicinity of the current electrodes to compute the apparent resistivity. The apparent resistivity is calculated as,

$$\rho_a = k \frac{V}{I} \quad 2\text{-}16$$

where *k* denotes the geometric factor with the dimension of length, *V* is the measured voltage and *I* is the applied current. The apparent resistivity is dependent on the geometry of the electrode array used. For example, the geometric factor for the Wenner array is calculated as (Reynolds, 1997):

$$k = 2\pi a \quad 2\text{-}17$$

where *a* is the electrodes spacing.

2.1.2.1 Application

The total number of 59 electrodes was installed in the column wall on the side opposite to the TDR probes at 3 cm intervals, starting from a height of 16 cm and ending at a height of 1.90 m. Resistivity measurements were conducted using Syscal Junior system and the collected data file was transferred to the PC using PROSYS software. To connect the electrodes to the Syscal, a system was designed which consist of binding posts, hook up wire (tinned copper, PVC insulated), a 2 m four-wire cable, and banana jacks. The binding posts were installed on a Plexiglas plate at 1 cm horizontal interval. A 2 m hook-up wire was used to connect each binding post to an electrode. The four-wire cable – which was connected to four banana jacks at both ends – connected the Syscal to the binding posts.

DC resistivity measurements performed using the Wenner array with constant electrode spacing of 3 cm to determine the vertical variability of the apparent resistivity. This method is called vertical

resistivity profiling (VRP). DC resistivity measurements were taken during the lowering and raising of the water level, as well as before and after each gasoline injection.

2.2 Experimental Procedure

2.2.1 Column Design

To investigate the geophysical response of gasoline spills under controlled conditions, an experiment was conducted using a cylindrical polyvinyl chloride (PVC) column, 2 m in height and 0.61 m in diameter (ID). As shown schematically in Figure 2-2, the column consists of two monitoring wells (#1 and #2), an injection well, TDR probes, resistivity electrodes, a vent, a lid, a manometer, a crossed SCH 40 well screen (0.010" slot and 1.25" diameter), an inlet/outlet system, and a water reservoir.

The crossed well screen, which would allow the uniform distribution of water, was placed inside the column at the bottom. The inlet/outlet system which consisted of a PVC pipe and a valve was attached to the crossed well screen from outside. The valve controlled the flow of water in and out of the column. The outlet was connected to the water reservoir through a Teflon tubing of 1/4" diameter. The manometer was installed on the outlet system to show the water level inside the column. The 61 TDR rods, 21.3 cm in length and 0.32 cm diameter, were installed at 3 cm increments in the column wall using plastic Swagelok® connectors. Resistivity electrodes, 3.5 cm length and 0.2 cm diameter were inserted at 3 cm intervals in the column wall on the opposite side from the TDR probes. The central PVC pipe (1.25" diameter and 1 m length) that was slotted over the lower 10 cm was used as the injection well. To keep a reasonable distance between the TDR probes and the injection well, the injection well was placed 5 cm off the center, toward the resistivity electrodes (Figure 2-3).

The two fully screened PVC (0.010" slot and 1.25" diameter) monitoring wells were installed to permit the measurement of the water level and the thickness of the free phase inside the column. Those wells were placed along the column wall approximately 90˚ from plane of the TDR rods-resistivity electrodes. The lid, which was also made of PVC, was used to prevent the release of gasoline volatiles in the laboratory, and the vent was installed to prevent the accumulation of volatiles inside the column. Pictures of the column are found in the Appendix B.

To ensure the quality of the column seals and to find the geometric factor for the electrode array used for resistivity method, the column was filled with water, and resistivity measurements were

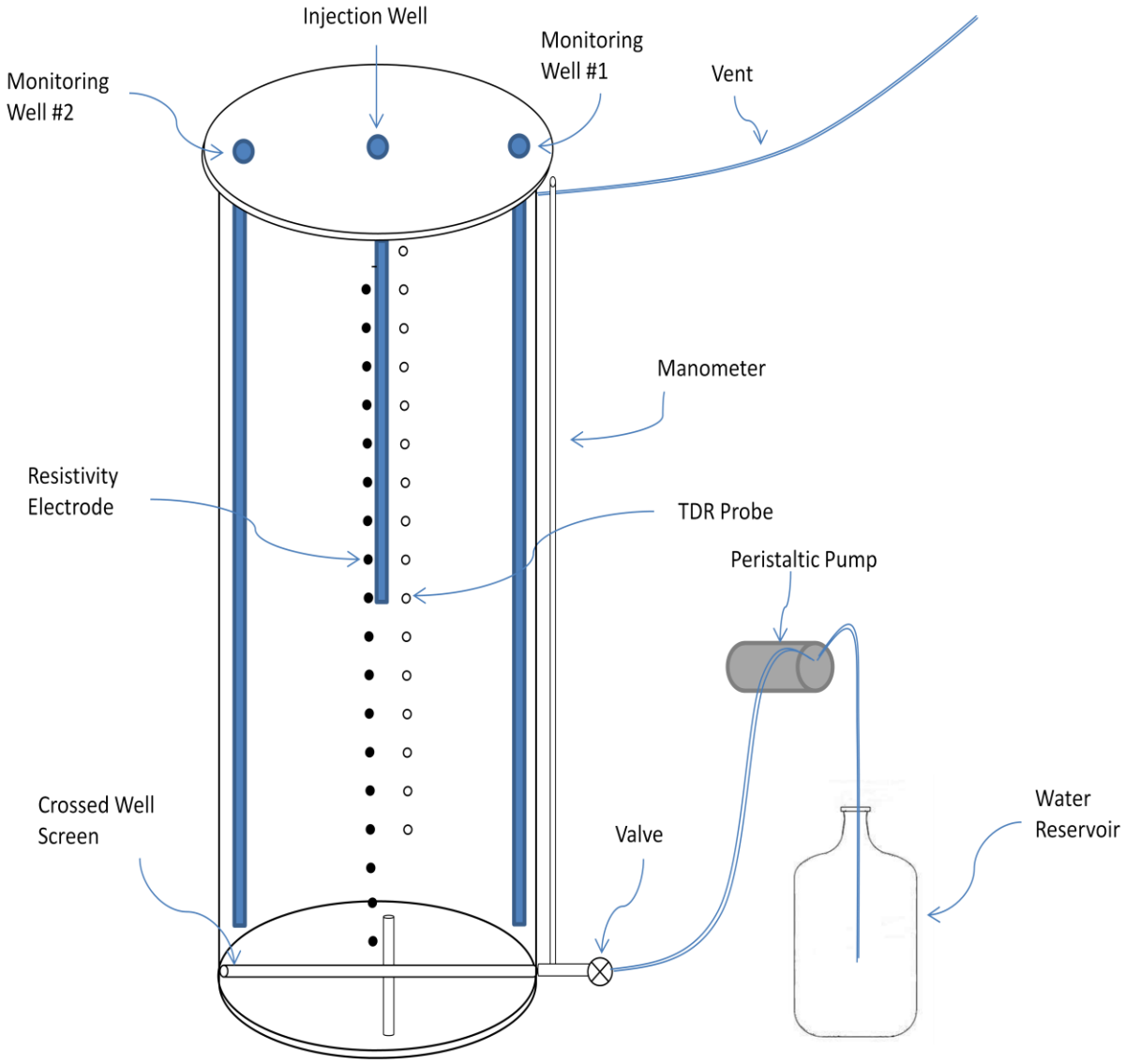

Figure 2-2 Schematic diagram of the column

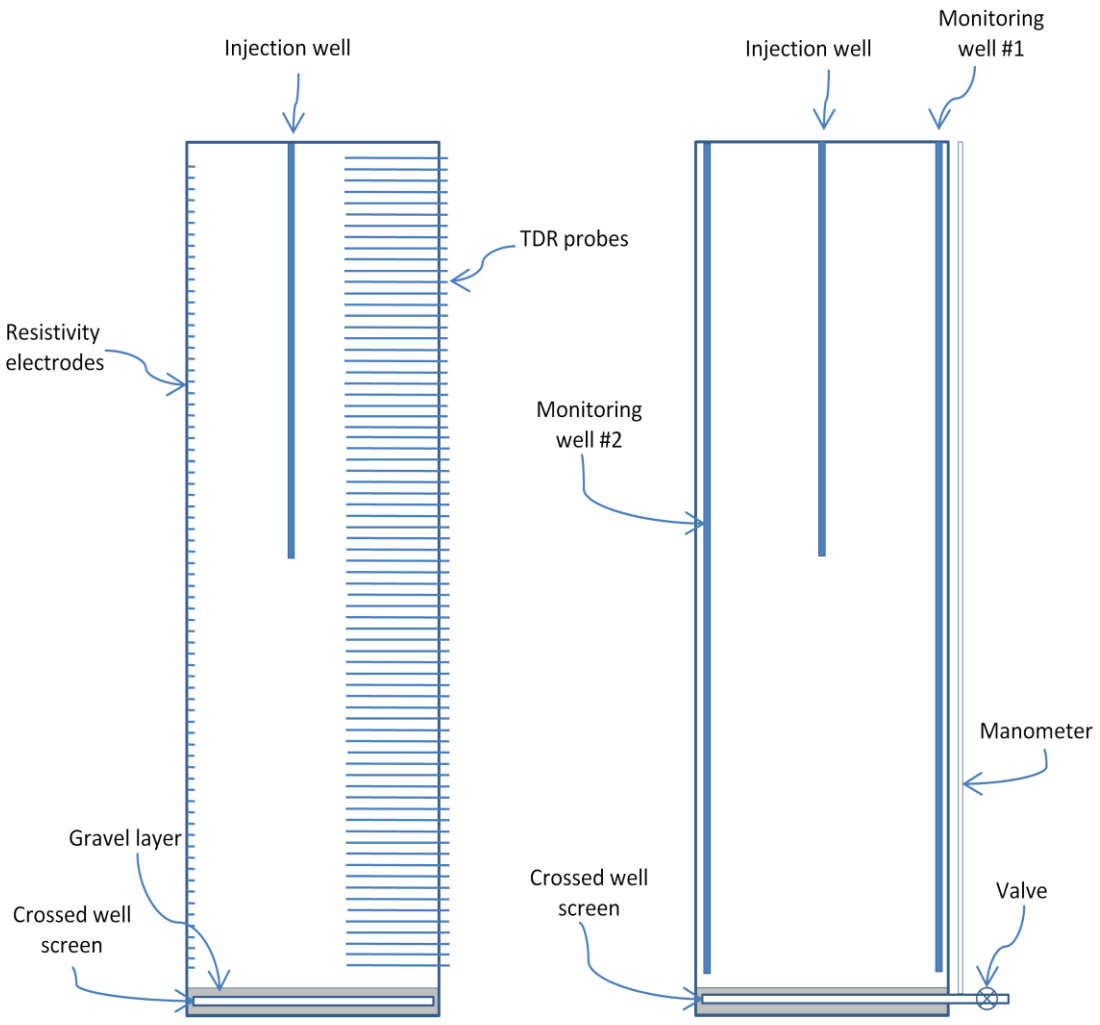

Figure 2-3 Diagram on the left side shows the cross section through geophysical instrumentation; right side diagram shows the cross section through the wells (perpendicular to the TDR rods-resistivity electrodes plane).

taken. Resistivity results indicated that the measured geometric factor for the electrode spacing was very close to that calculated for a Wenner array at the surface of a half space (Appendix A).

2.2.2 Packing and Saturation Procedure

Before the packing was started, all of the electrodes and TDR rods were removed. To maintain good hydraulic conductivity, the crossed well screen at the bottom of the column was covered by 10 cm of pea gravel. The filling material for the rest of column consisted of the much studied Borden sand, which was brought from the uncontaminated part of the site. The sand was dried at room temperature and then sieved through a 2 mm mesh to remove the leaves and roots. The column was incremental packed in 5 cm layers. The sand was damped prior to packing to prevent grading of the sand grains while it was poured into the column. A hand tamper consisting of a heavy metal plate attached to a 2 m long handle was used to pack each sand layer (Figure 2-4 a). Before the next layer of the sand was added, the surface of the existing layer was raked to prevent stratification (Figure 2-4 b). The monitoring wells were placed in the sand at a height of 15 cm (5 cm above the gravel layer). The injection well was placed at a height of 1.05 m at the midpoint between the two monitoring wells. The column was packed to a height of 1.96 m. After the packing was completed, all of the TDR rods and electrodes were re-introduced to the system.

Air bubbles entrapped within the porous medium decrease the water saturation of the soil. A method to enhance the saturation process is to replace the air in the pores with CO_2 before the saturation process is begun. Since CO_2 is highly water-soluble, any CO_2 bubbles entrapped in the pores will dissolve quickly in the water. Hence, CO_2 gas was flushed through the column at a pressure of 20 psi for 3 days. Subsequently, tap water, which was stored in a 50 L container to de-air the fluid, was pumped into the bottom of the column using a peristaltic pump at a low flow rate of 15 ml/min for 17 days. The low flow rate was intended to increase the probability that all of the pores are filled with water. The total water used to fill the column was ≈ 140 L.

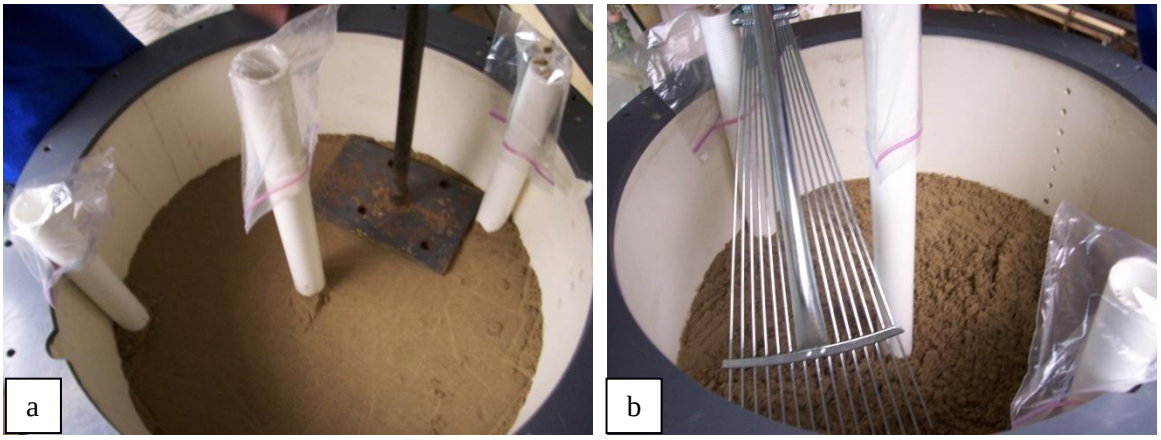

Figure 2-4 a: Packing the sand using a hand tamper; b: raking the surface of the sand to prevent stratification during the packing.

After the sand became fully saturated, TDR and resistivity measurements were conducted to obtain the background permittivity and conductivity profiles. These initial measurements indicated that uniform conditions had not been attained in the column. As shown in Figure 2-5, the soil conductivity is low (≈ 19 mS/m), in the bottom portion of the column up to a height of 40 cm. It then increases gradually up to a height of 70 cm and remains fairly constant around 48 mS/m to the top of the column. In contrast, TDR measurements (Figure 2-6) indicated that the permittivity, which has a direct relationship with water content, had a higher value up to a height of 65 cm and decreased slightly to the top of the column.

To achieve uniform background electrical conductivity and dielectric permittivity before starting the experiment, water was circulated upward through the column. Hence, water was pumped into the base of the column with a peristaltic pump at a flow rate of a 30 ml/min; and, a siphon was installed in the column wall above the soil surface to collect the outflow. The conductivity front was moving upward about 6 cm a day.

After 53 days of circulation of water, the flow rate was increased from 30 ml/min to 97 ml/min and consequently the movement of the conductivity front tripled to ≈20 cm a day. After two weeks, the flow rate was increased to 125 ml/min for 23 days. In total, about 5000 L water was circulated through the column for 90 days. During this process, both the electrical conductivity and dielectric permittivity were monitored; these profiles are shown in Figures 2-7 and 2-8, respectively. It can be

seen that condition in the column became progressively more uniform during the circulation procedure. After 90 days, conditions appeared to have stabilized and further potential improvement in column uniformity were deemed to be relatively minor. Hence, resulting conditions were taken to be the baseline water-saturated reading for the column.

The reason for anomalous electrical conductivity and permittivity is not clear, but we thought that the reason could be a chemical reaction inside the column. Therefore, two samples from the water inside the container (one before tap water was added, one after tap water was added) which was pumped into the column, and one sample from water coming out of the siphon was collected and analyzed for cations and anions, pH and alkalinity. However, the result showed that there are no significant differences between these three water samples.

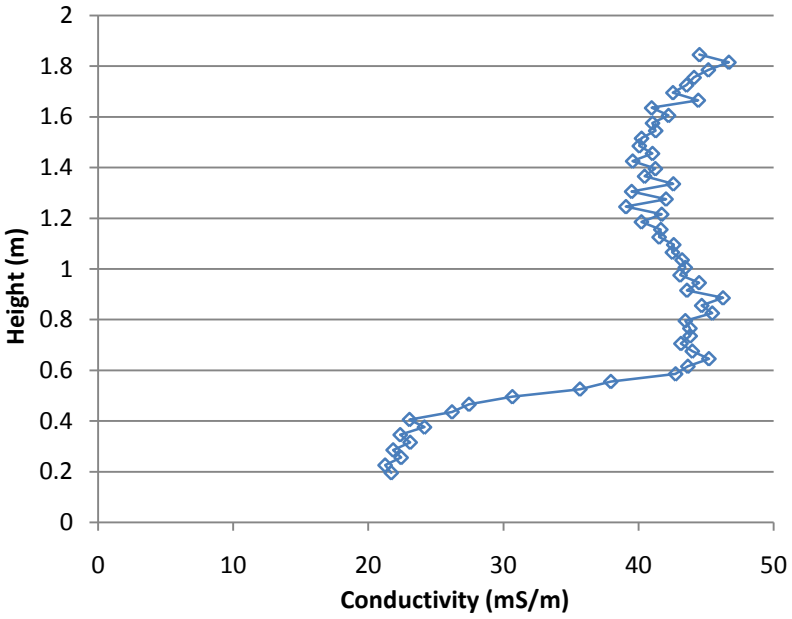

Figure 2-5 Conductivity profile after the initial saturation process was completed.

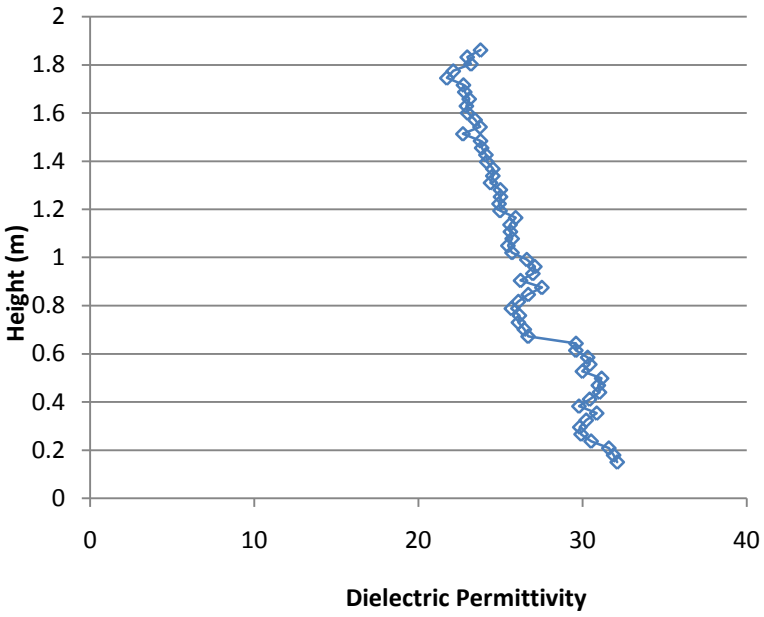

Figure 2-6 Dielectric permittivity profile after the initial saturation process was completed.

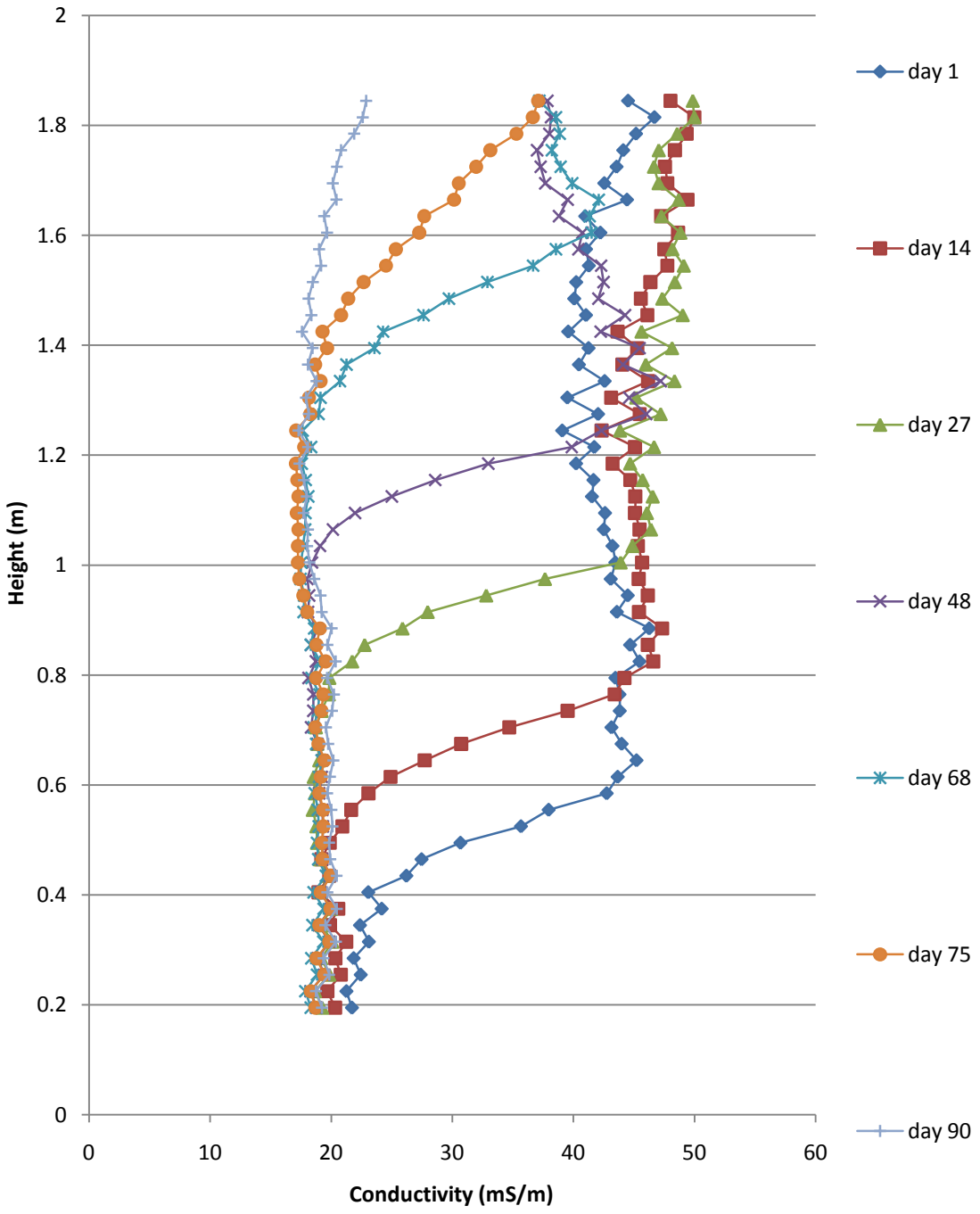

Figure 2-7 Electrical conductivity profiles obtained from the VRP measurements during the 90 days water circulation period.

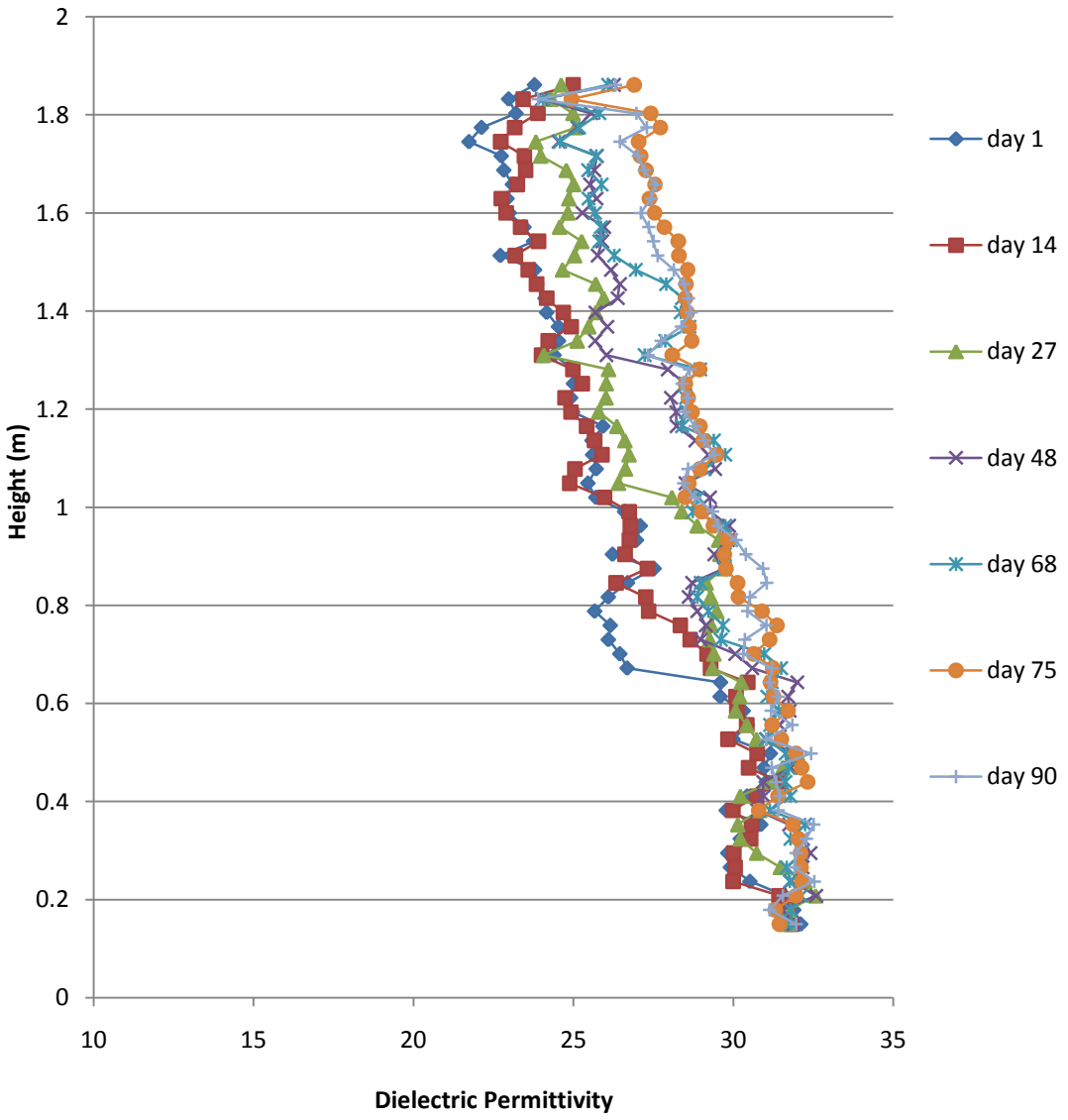

Figure 2-8 Dielectric permittivity profiles obtained from the TDR measurements during the 90 days water circulation period.

2.3 Chronology of the experiment

Following the establishment of the initial conditions, a series of water level changes and gasoline releases were performed and geophysically monitored. The timetable of these steps during the experiment is provided in Table 2-1and in the next chapter, those step and associated experimental results will be discussed in detail.

Table 2-1 Timetable of the experiment

Day	Steps	VRP and TDR Measurements
1 to 13	Lowering the water level to a height of 0.73 m	4 measurements for each method on days 5, 7, 9, and 11 while lowering the water level; and 1 measurement for each method on day 13 after equilibration.
13	Spill of 1 liter of gasoline	before the spill, 0.5, 1, 4, 7 hours, and 1, 3 days after the spill
16	Spill of 2 liters of gasoline	before the spill, 0.5, 2 hours, and 2, 3, 5, 6 days after the spill
22	Spill of 2 liters of gasoline	before the spill, 0.5, 6.5 hours, and 3, 5, 6, 10 days after the spill
54 to 75	Raising the water level to a height of 1.02 m	6 measurements for each method on days 54, 55, 56, 57, 61, and 62 while raising the water level; and 3 measurements for each method on days 64, 67, and 75 while equilibrating.
75 to 103	Lowering the water level back to the original level (0.73 m)	5 measurements for each method on days 76, 77, 78, 91, and 92 while lowering the water level; and 1 measurement for each method on day 103 after equilibration.
103	Cores A and B	
110 to 124	Lowering the water level to a height of 0.43 m	1 measurement for each method on day 110 before lowering the water level; 6 measurements for each method on days 112, 114, 116, 117, 118, and 119 while lowering the water level; and 1 measurement for each method on day 124 after equilibration.
124 to 132	Raising the water level back to the original level	4 measurements for each method on days 125, 126, 128, and 132 while raising the water level.
140	Cores C and D	

Chapter 3
Experimental Results

For this experiment, gasoline was to be injected into the transition zone (the zone above the capillary fringe in which water saturation decreases rapidly) to investigate the geophysical response of the unsaturated zone and capillary fringe to the gasoline spill. Therefore, it was necessary to lower the water level within the column until the top of the capillary fringe was positioned immediately below the injection well screen. Lowering of the water level took place over an 11 day period. To minimize the disturbance of the system and permit adequate drainage of the medium, the water level was lowered by removing water at a very low flow rate of 10 ml/min for 6 to 8 hours a day. As a result, the water level was lowered by 18 to 20 cm each day of pumping. It was observed that the water level recovery of 5 to 6 cm occurred overnight before commencing the pumping on the following day. Geophysical measurements were taken every other day before the pumping resumed (Figures 3-1 and 3-2). As can be seen in the figures, both the VRP and TDR profiles undergo vertical translations as the water level is lowered, indicating systematic drainage of water.

The water level was lowered to a height of 68 cm on day 11 and recovered by 5 cm to stabilize at a height of 73 cm. At this point, the top of the capillary fringe was located approximately 5 cm below the injection well screen. The system was allowed to equilibrate a further two days prior to start of the gasoline release.

3.1 Gasoline Injection

Standard API 91-01 gasoline was released into the column in three steps; the amount of gasoline injected in the first, second, and third steps were 1, 2, and 2 liters, respectively. The progressive injection of gasoline allowed the evaluation of the response of geophysical methods to increasing amount of gasoline. In addition, the water table elevation was maintained at 73 cm during the injection phase of the experiment. This condition was achieved by attaching one-meter length of 1/4" Teflon tubing to the outlet and fixed the other end at the desired height of 73 cm.

The first release took place on day 13 with the injection of 1 liter of gasoline into the column. VRP and TDR measurements were taken before the spill, and 0.5, 4, and 7 hours, and 3 days after the spill. The cumulative effluent water on the 3 days after the first spill was 3.39 liters, of which 1 liter drained within the first hour after the spill. The cumulative volume of the effluent water was more

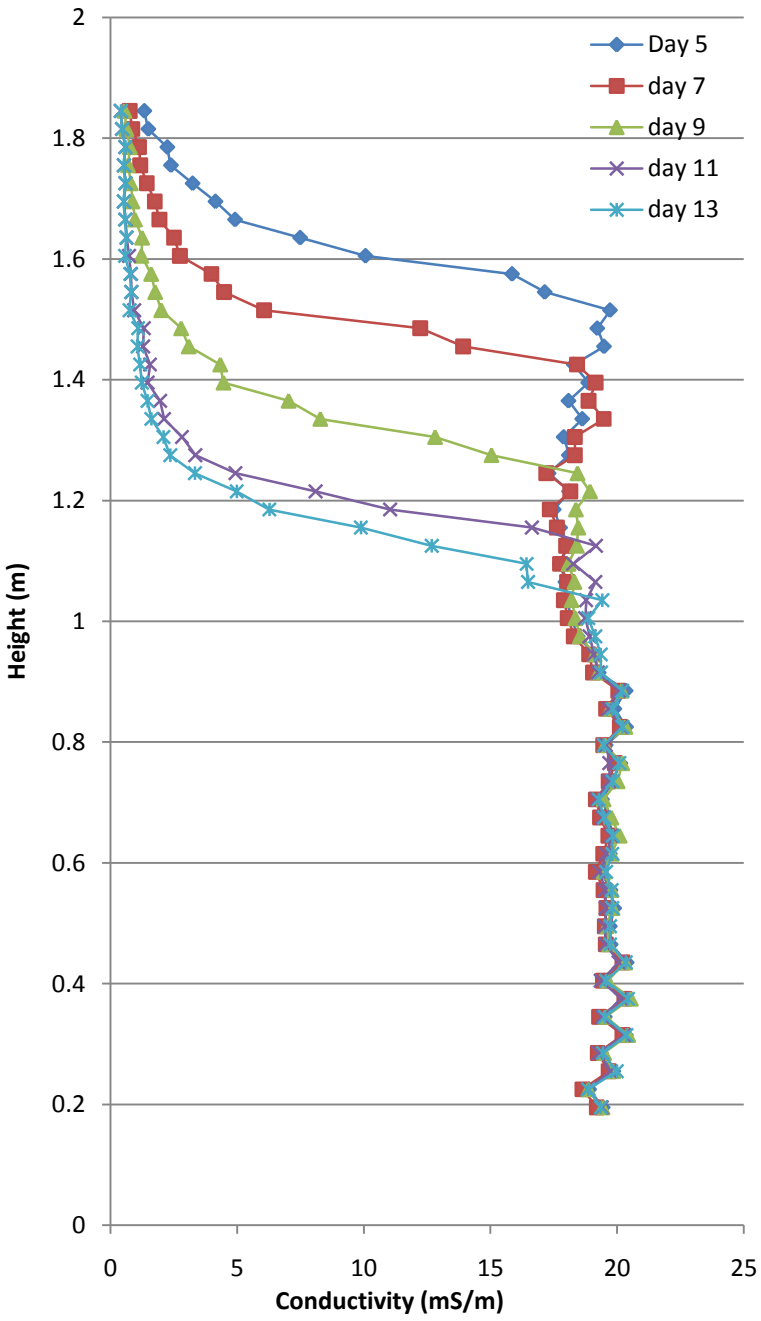

Figure 3-1 Translation of electrical conductivity profile obtained from VRP measurements during the period of lowering the water level prior to the injection

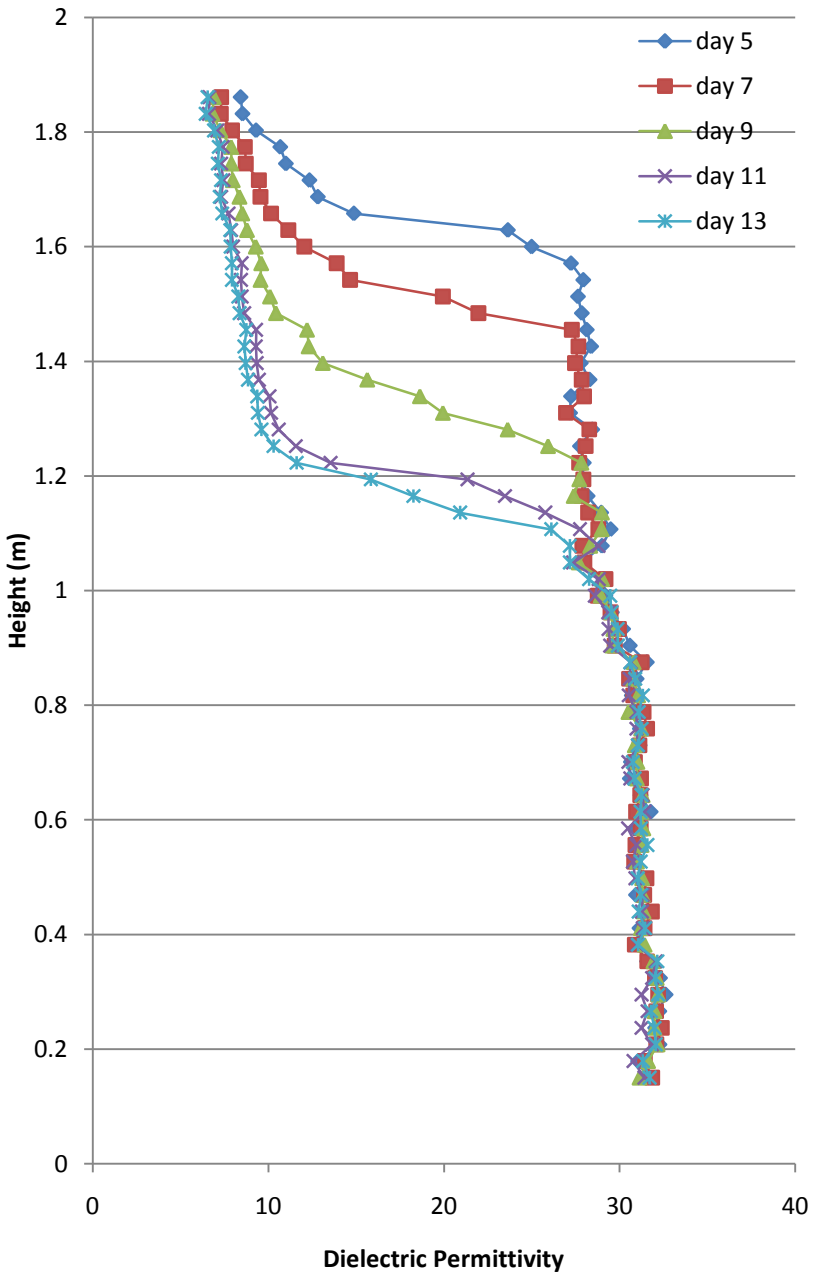

Figure 3-2 Translation of dielectric permittivity profile obtained from TDR measurements during the period of lowering the water level prior to the injection

than 3 times the volume of the injected gasoline. This effect can be explained by the reduction of the capillary fringe thickness due to the decrease in the surface tension due to the presence of the organic compounds. Before the release, capillary fringe thickness was estimated to be approximately 31 cm, as the geophysical instrumentations indicated that full saturation occurred to a height of around 104 cm, while the height of the actual water table in the manometer was 73 cm. This capillary fringe thickness is comparable with the average thickness (30 cm) estimated by Bevan et al. (2005) during the field study of the Borden sand. Comparison of the before and after release profiles for the VRP conductivity measurements (Figure 3-3) show that the capillary fringe thickness was decreased by ~ 5 cm due to the first gasoline injection, while the TDR permittivity profiles before and after release (Figure 3-4) show that the capillary fringe thickness was reduced by 8 cm. Perhaps, the amount of gasoline was not enough to reach the edges of the column, and because the sampling volume of the VRP electrodes is much smaller due to the smaller length than the TDR probes, the VRP measurements showed less decrease in the capillary fringe thickness. The minor change in trend of pre-release dielectric permittivity and conductivity profiles at a height of 1.05 m (marked with an open circle on Figures 3-3 and 3-4), which corresponds to the beginning of the injection well and might be an indication of different packing at the time the injection well was installed. As can be seen in the figures, desaturation of the soil occurred from that point.

The system was allowed to equilibrate for 3 days after the first injection and 2 additional liters of gasoline was injected into the column on day 16. VRP and TDR measurements were taken before this release and for 6 days after the spill (Figures 3-5 and 3-6). Both figures show that the dielectric permittivity and electrical conductivity values progressively decrease over time as more gasoline (which has lower electrical conductivity and dielectric permittivity than water) gradually penetrates the pores. The similar profiles for days 5 and 6 indicate that the system was approaching equilibrium. The additional effluent water 6 days after the second spill was 4.65 liters, of which 1 liter drained within 30 minutes after the second injection. The cumulative volume of the effluent water was more than twice the volume of the injected gasoline. The conductivity profiles before the second spill and 6 days after the spill indicate that the thickness of the capillary fringe decreased by a further 7 cm, but the permittivity profiles show a reduction of about 9 cm, indicating that gasoline did not reach the edges yet.

The third injection took place on day 22, when a final 2 liters of gasoline was injected into the column. Measurements were taken before the spill; and until 10 days after the spill. As shown in

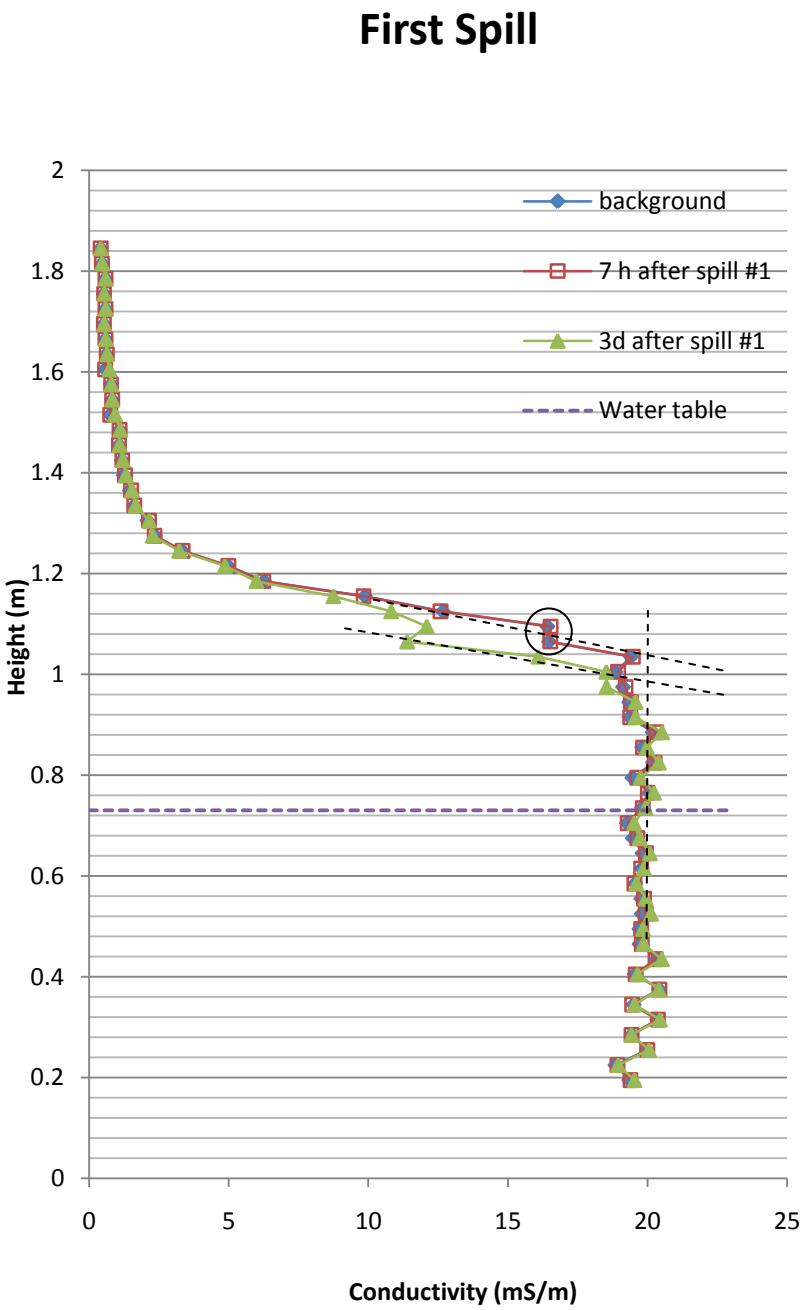

Figure 3-3 Electrical conductivity profiles obtained from the VRP measurements before and after the first gasoline injection. The background profile, which refers to the uncontaminated sand, is overlaid by 7 hr. after spill data.

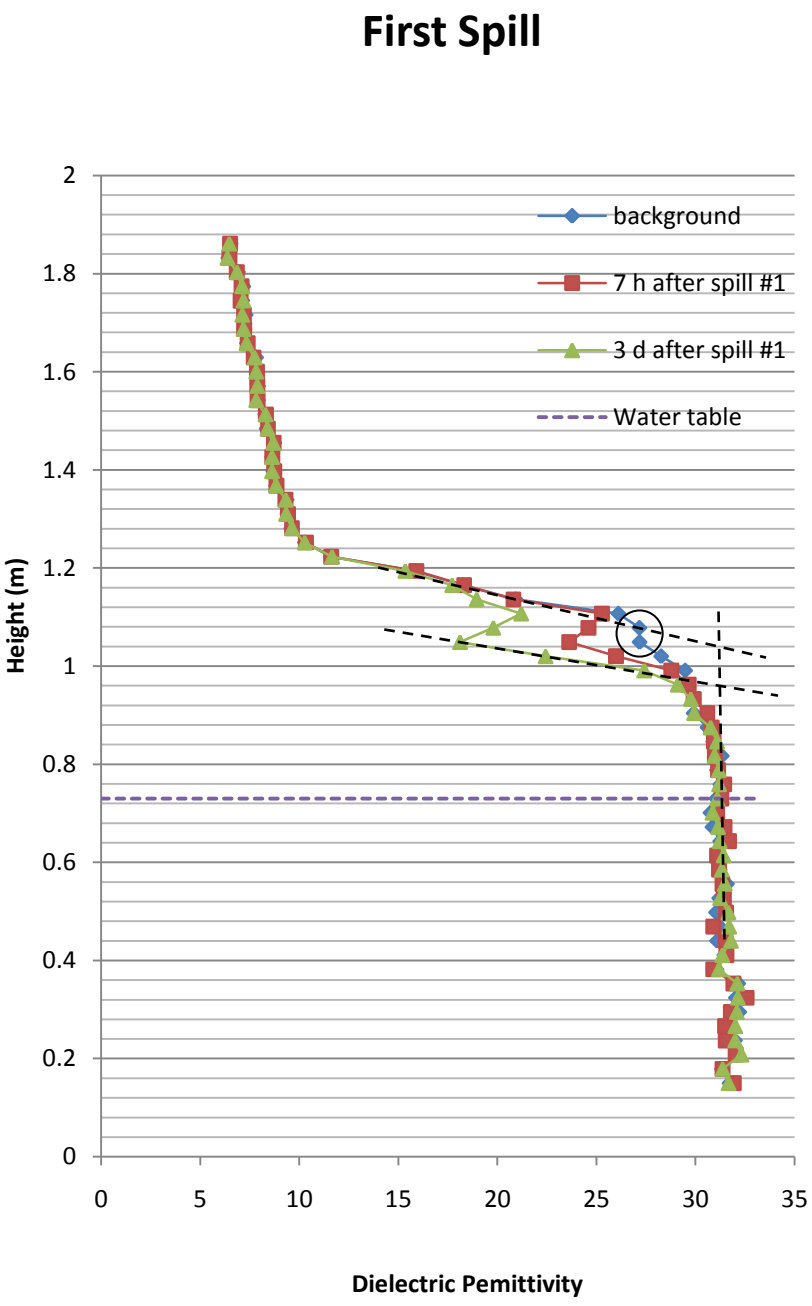

Figure 3-4 Dielectric permittivity profiles obtained from TDR measurements before and after the first gasoline injection. Background profile refers to the uncontaminated sand.

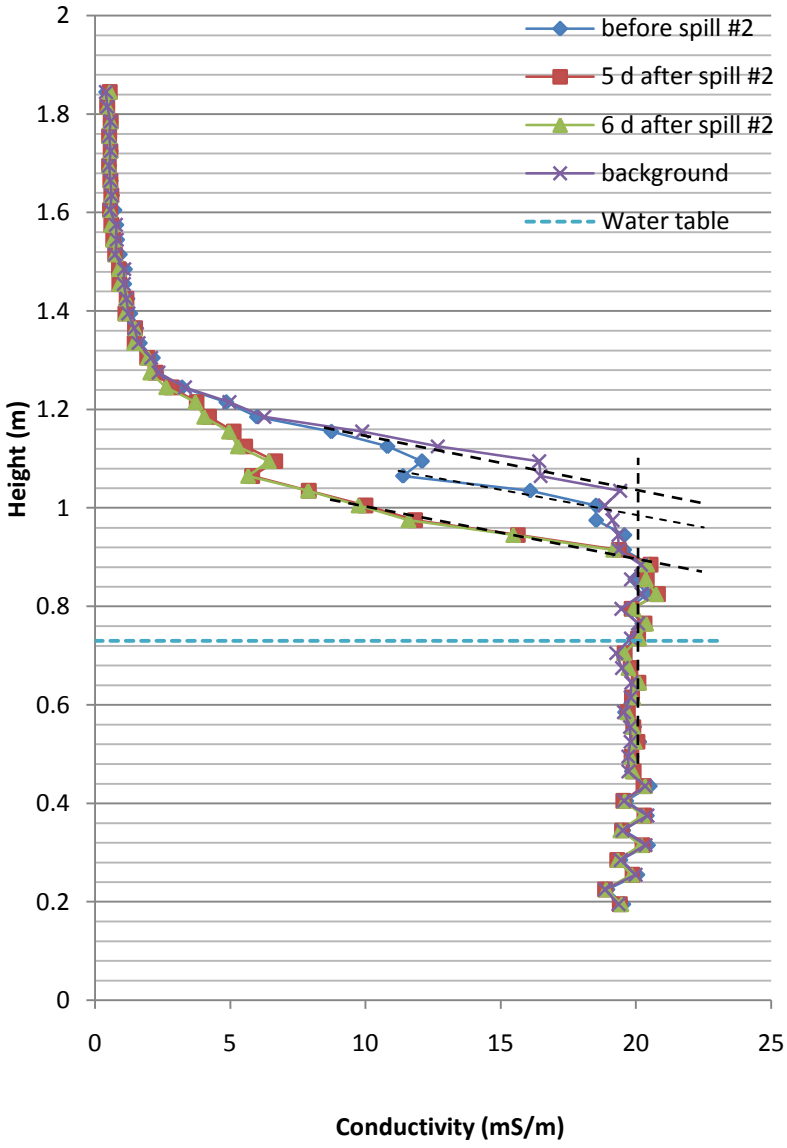

Figure 3-5 Electrical conductivity profiles obtained from the VRP measurements before and after the second gasoline injection. Background profile refers to the uncontaminated sand.

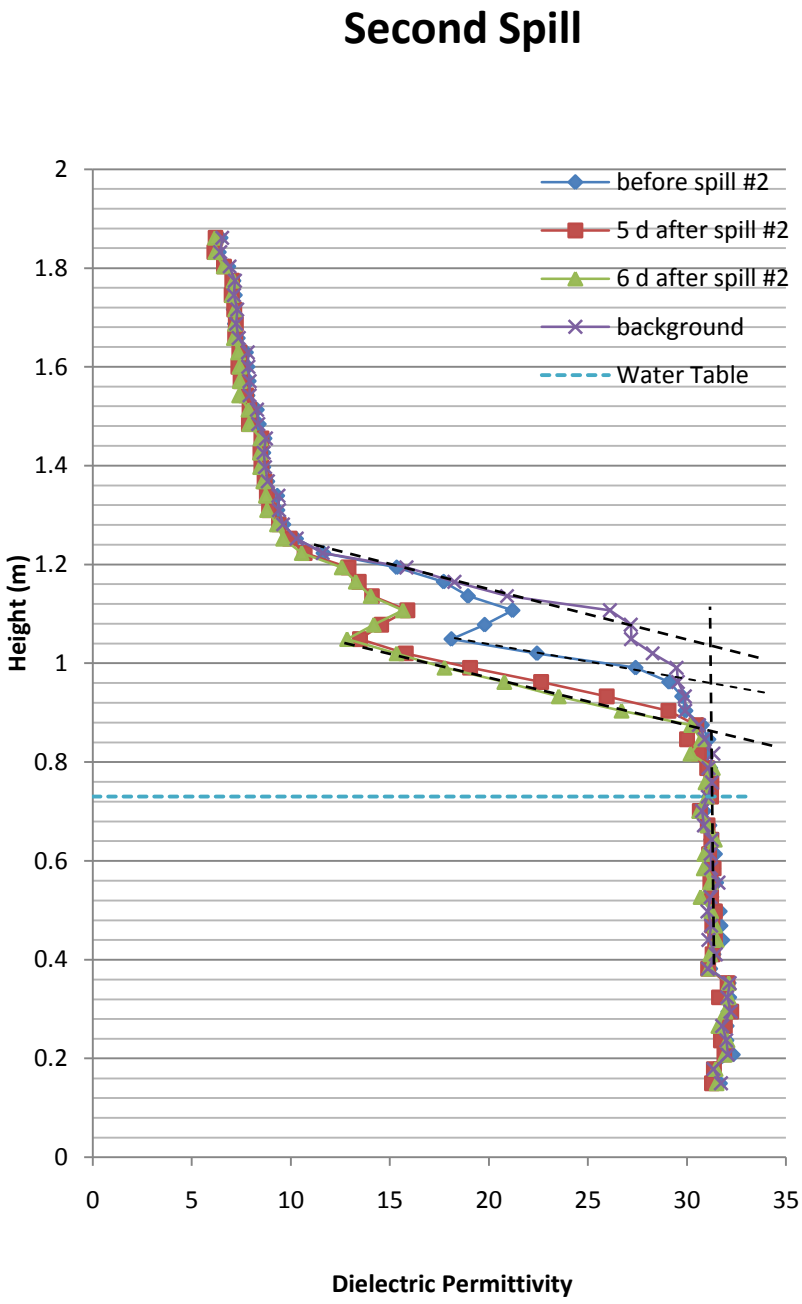

Figure 3-6 Dielectric permittivity profiles obtained from TDR measurements before and after the second gasoline injection. Background profile refers to the uncontaminated sand.

Figures 3-7 and 3-8, there is a small change in electrical conductivity and dielectric permittivity profiles before and after the third spill. The additional effluent water on the 10 days after the third spill was 2.1 liters (almost identical to the volume of injected gasoline), of which 1 liter drained within 30 minutes after the third spill. The conductivity profile before the third spill and 6 days after the spill indicates that the capillary fringe thickness decreased by additional 5 cm; however, the permittivity profiles indicate that the capillary fringe thickness did not changed. Probably, after the third spill, gasoline reached the edges of the column. In total, both geophysical profiles show that the capillary fringe thickness decreased by 17 cm after three steps of gasoline injection.

On day 10 after the third spill, the thickness of gasoline in the two monitoring well was measured. Unexpectedly, there was 60 cm gasoline in monitoring well #1 and a thin layer of gasoline (about 2 mm) in the monitoring well #2. Further, comparison of the electrical conductivity and permittivity profiles obtained after the second and third injection show only minor changes. Hence, it appears that there is a preferential gasoline flow path established after the third release in the direction of monitoring well #1 through which most of gasoline added to the system during this final injection migrated to the well.

At this point, an attempt was made to remove the excess gasoline from monitoring well #1 before proceeding with the next portion of the experiment. The total amount of 1640 ml of gasoline was pumped from the monitoring well #1 over a period of 14 days between days 32 to 46. Geophysical measurements showed that the conductivity and permittivity profiles did not change before and after removing the gasoline (Figures 3-9 and 3-10). The thickness of the gasoline layer in the well #1 measured on day 46 was 1 cm. The water level elevation inside the well #1 was 70 cm and inside the well #2 was 73 cm. After the last step of removing gasoline from the well on day 46, the system was allowed to equilibrate for 8 days. During this period, the thickness of the gasoline layer in the well #1 was increased to 16 cm. At the time, the water level elevation inside the well #1 was 60 cm and inside the well #2 was 73 cm.

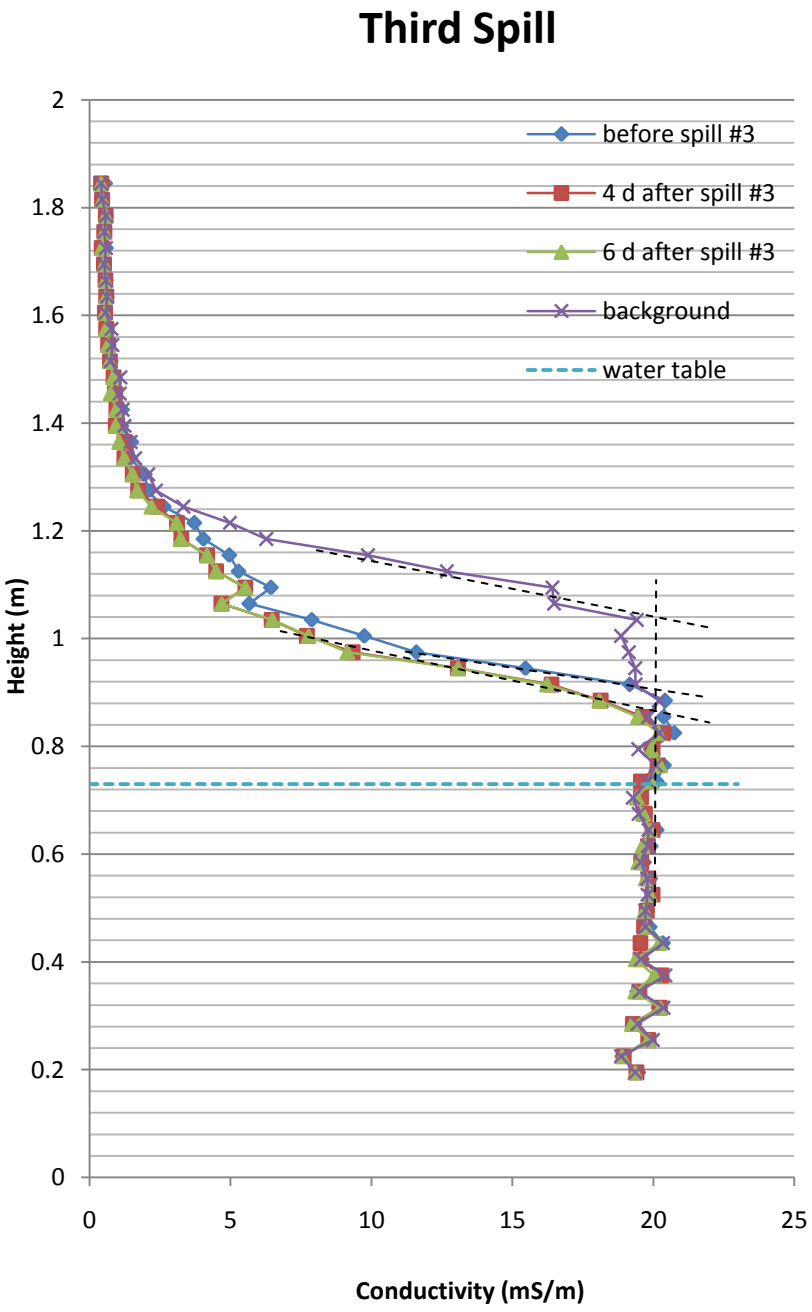

Figure 3-7 Electrical conductivity profiles obtained from the VRP measurements before and after the third gasoline injection. Background profile refers to the uncontaminated sand.

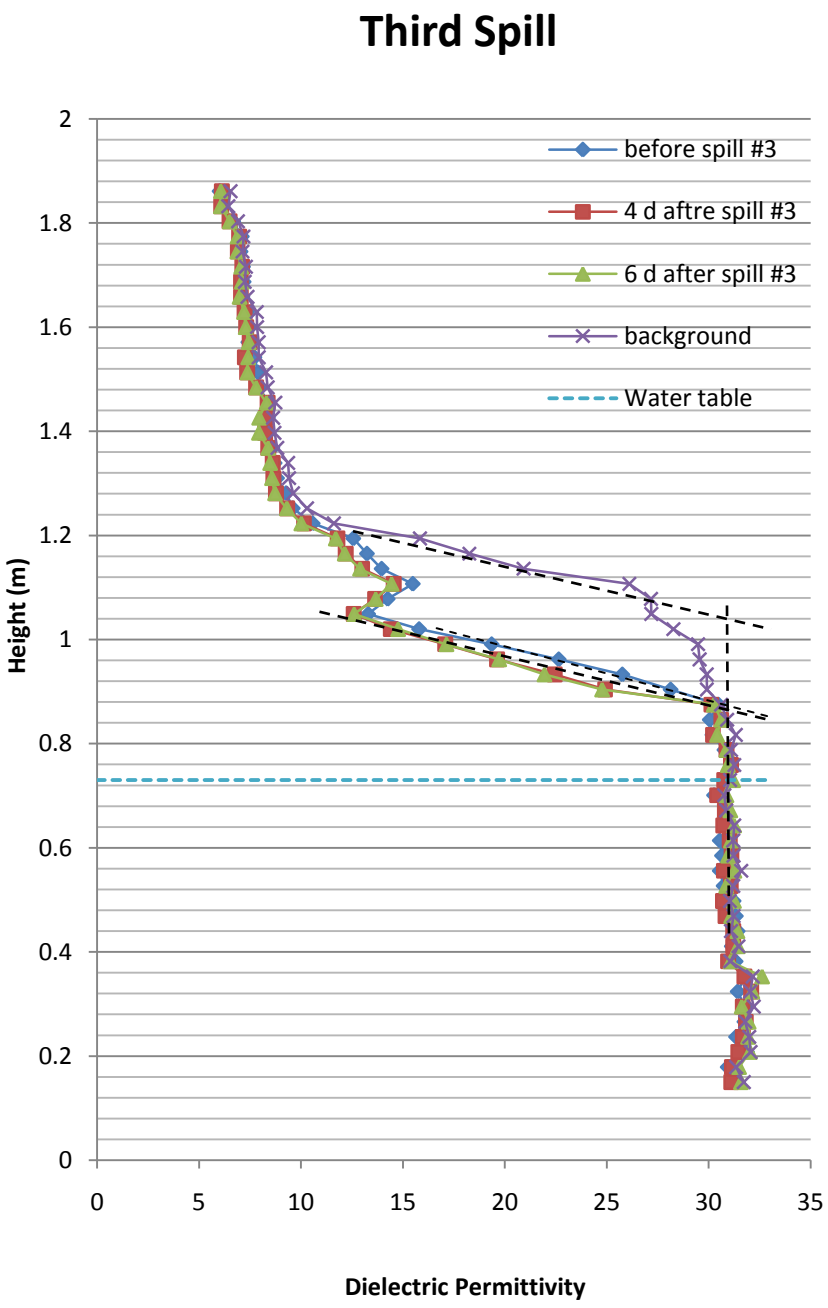

Figure 3-8 Dielectric permittivity profiles obtained from TDR measurements before and after the third gasoline injection. Background profile refers to the uncontaminated sand.

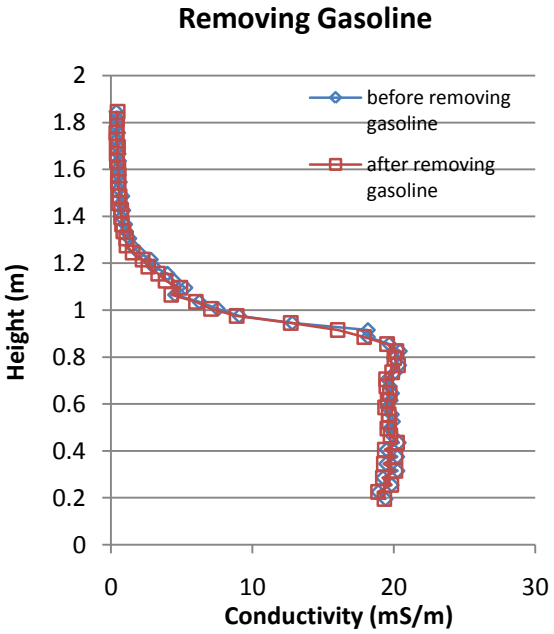

Figure 3-9 Electrical conductivity profiles obtained from VRP measurements before and after removal of the 1640 ml of gasoline from monitoring well #1.

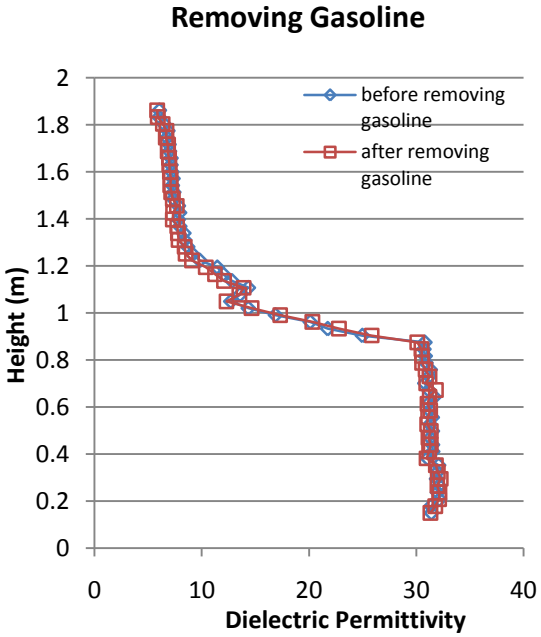

Figure 3-10 Dielectric permittivity profiles obtained from TDR measurements before and after removal of the 1640 ml of gasoline from monitoring well #1.

3.2 Water Table Fluctuation 1

In nature, the water table fluctuates due to the precipitation and evaporation during each season; these water table fluctuations act as imbibition and drainage mechanisms. During imbibition, a wetting phase such as water displaces a non-wetting phase such as air or NAPL. In contrast, displacement of a wetting phase by a non-wetting phase is called drainage. The pore structure (e.g., pore size distribution) controls the fluid saturations that result from these two processes.

To investigate the geophysical responses to the entrapped gasoline, the water level within the column was first raised and then lowered to its starting elevation. Water was pumped into the column using a peristaltic pump at a very low flow rate of 6 ml/min, for a period of 5 to 6 hours a day. Raising the water level took place from day 54 to day 62 and system was allowed to equilibrate until day 75. VRP and TDR measurements were taken before each rising of the water level and during the equilibration period (Appendix B). On the first 2 days water level was rose relatively fast (6.5 cm in 5 hours). During this time, the thickness of the gasoline layer in the monitoring well #1 increased from 16 cm to 22 cm on the first day and to 28 cm on the second day, indicating that water moved through the contaminated zone, displacing gasoline that migrated to the well along the established preferential flow path.

Water level continued to rise at a significantly slower rate from since the third day onward (e.g., 2.9 cm in 6 hours on day), while the thickness of the gasoline layer in monitoring well #1 remained fixed at 28 cm. Water level was eventually raised to a height of 1.14 cm on day 60, after which point the system was allowed to equilibrate for two weeks. During this equilibration period, the water level dropped by 12 cm and established itself at a height of 1.02 m. In total, the water level was raised about 29 cm by adding 16 liters of tap water.

When water moves through the gasoline contaminated zone, depending on the pore structure, gasoline will be displaced by water to some extent. The zone in which the soil contains both immiscible fluids (LNAPL and water) due to the water level variations is called a smear zone. The conductivity and dielectric permittivity of the smear zone are higher than those of the contaminated zone due to the presence of water. Figures 3-11 and 3-12 show the electrical conductivity and dielectric permittivity of the soil during the first fluctuation cycle. As can be seen in the figures, electrical conductivity and TDR permittivity of the soil increased after raising the water level to a height of 1.02 m, but did not reach the values of a full-water saturation zone. The intermediate conductivity and permittivity values in the overlying zone to approximately 1.20 m elevation (Figures

3-11 and 3-12) indicate the presence of an entrapped gasoline phase in the newly created capillary fringe. The geophysical response above 1.20 m for the raised water level case is that of air-water system, because the trend of the profiles above 1.20 m is similar to the trend of the profiles for the lowered water level case before contamination (Figures 3-1 and 3-2).

To complete the first fluctuation cycle, the water level was lowered to its original level (73 cm). This step was achieved using a peristaltic pump running at a flow rate of 6 ml/min for 6 to 7 hours a day to remove water from the system. The water level was lowered starting on day 75 in five steps. Before starting each step, the thickness of the gasoline layer and depth to the water table in the monitoring wells, and conductivity and permittivity of the soil were measured. Thickness of the gasoline layer inside the monitoring well #1 was 28 cm for the first two days. Once the water level reached the original smear zone on the third day, the thickness of the gasoline layer increased to 29 cm, indicating that water displaced some of the gasoline during the drainage. The thickness of the gasoline increased to 33 cm on the next step of lowering the water level and remained the same while water was moving through the capillary fringe in which no gasoline exists in the pores. Water table stabilized at a height of 0.72 m one day after the last lowering step. The conductivity and permittivity profiles after lowering the water level back to its original level (Figures 3-11 and 3-12) match those before water table fluctuation. Although the break in the trend of the electrical conductivity and permittivity profiles can be an indication of the presence of a liquid with electrical conductivity and dielectric permittivity values lower than those values of water, VRP and TDR methods are not able to detect the redistribution of gasoline phase after the cycle and need to be combined with other methods such as soil core sampling.

3.3 Coring 1

Once the system reached equilibrium on day 103, two cores, A and B, were taken from the area between the monitoring well # 2 and the TDR rods, and Monitoring well #1 and the resistivity electrodes, respectively (Figure 3-13). The aim of core sampling was to provide the hydrocarbon profile across the soil and compare it to the conductivity and permittivity profiles. The cores were obtained manual from the surface of the sand to the depth of 1.3 m using 1.25" diameter aluminum tubing. Two cores of 25 cm in length were taken from the first 50 cm of the soil that was not contaminated. The rest of the cores were 15 cm in length. Short core samples were obtained as they are more representative of the soil texture; longer cores experience more soil compression inside the tubing, which alters its apparent depth. Since recovery of the core sample from the saturated sand is

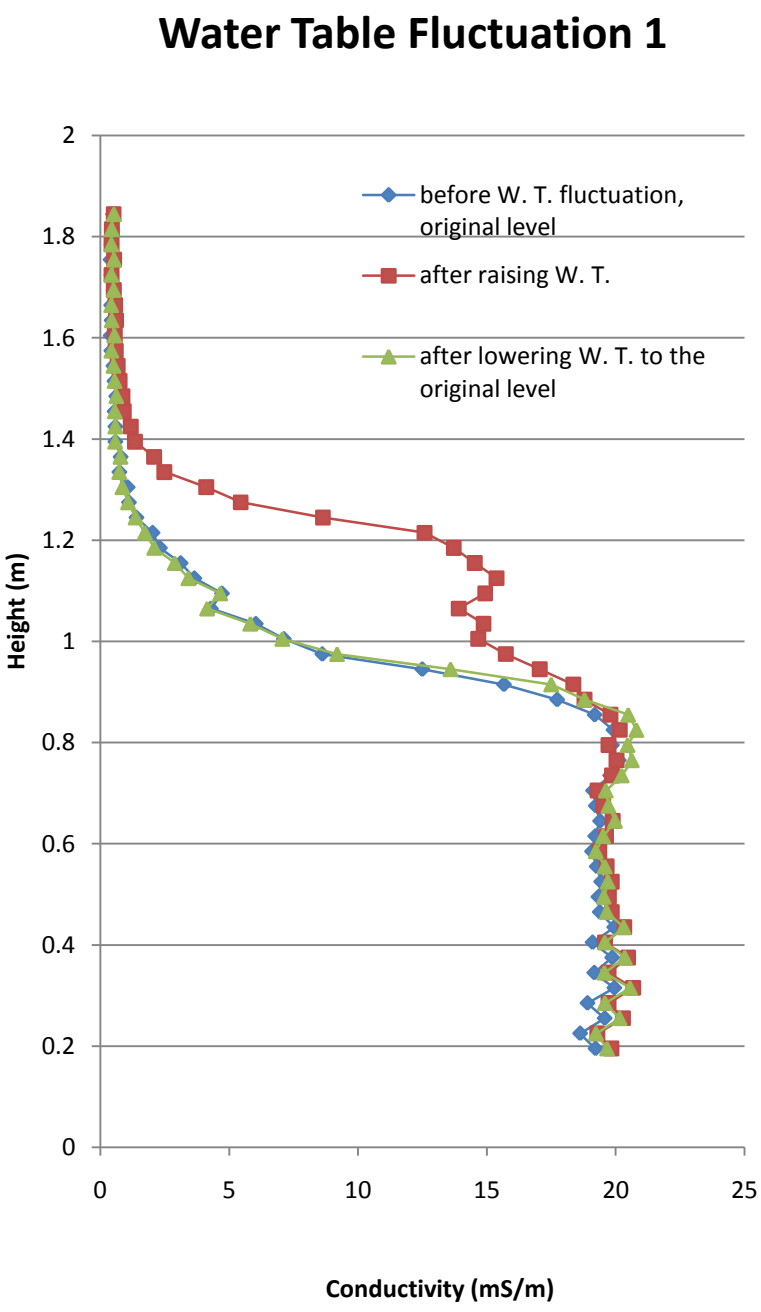

Figure 3-11 Electrical conductivity profiles obtained from VRP measurements during the first water fluctuation; W.T. stands for water table.

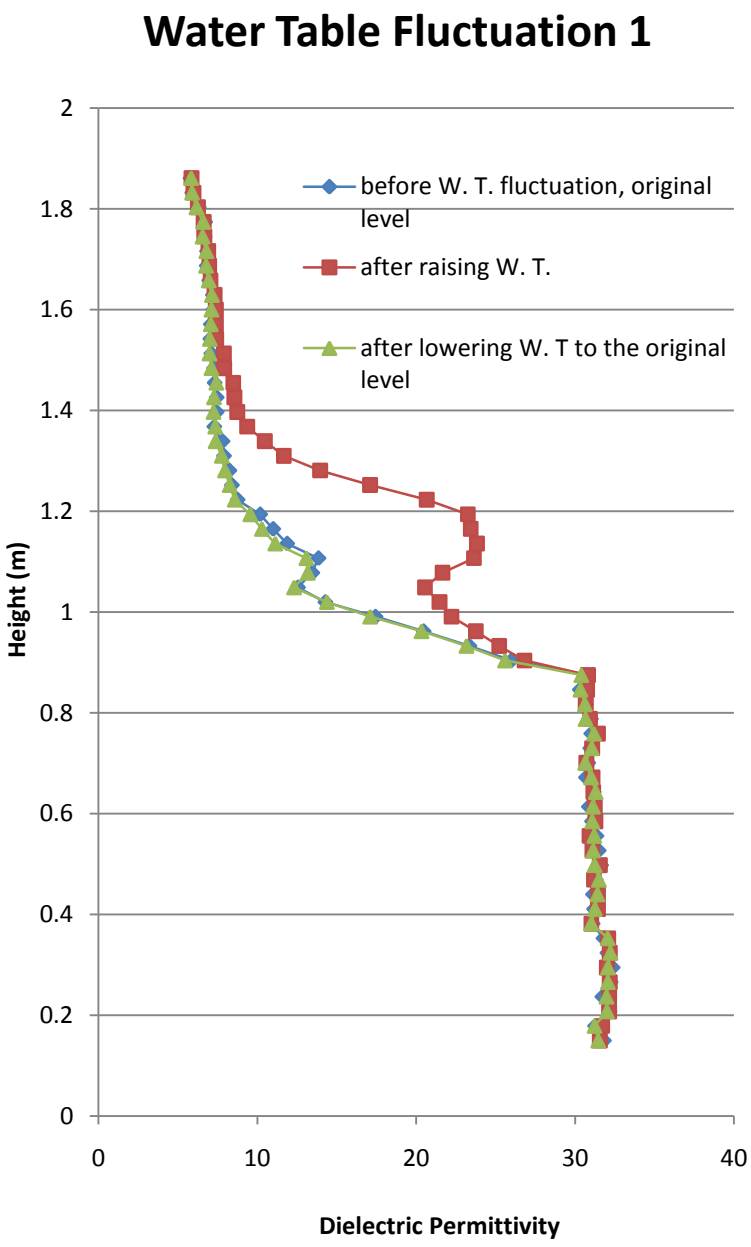

Figure 3-12 Dielectric permittivity profiles obtained from TDR measurements during the first water fluctuation; W.T. stands for water table.

difficult due to the gravity drainage of water and sand, the last core sample, which was from the capillary fringe and saturated zone, was taken using a piston sampler (Starr and Ingleton, 1992). The sampler consists of aluminum tubing, a piston inside the tubing, and a rod that controls the motion of the piston. Piston holds the soil inside the aluminum tubing by creating a vacuum above the soil core.

Each core sample was cut into 3 cm segments and about 5 g of soil from each segment was put into a Teflon® screw cap vials (20 ml) containing 5 ml of methylene chloride. The samples were shaken vigorously for 14 hours to extract all of the gasoline adsorbed to the soil grains and then analyzed for total petroleum hydrocarbon (TPH) in the Organic Geochemistry Laboratory at the University of Waterloo. In total, 40 samples were obtained from core A and 42 samples were obtained from core B.

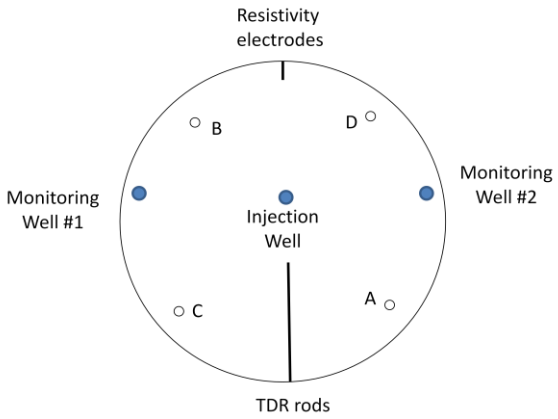

Figure 3-13 Cross section of the column showing the location of the cores taken from the sand

To compare the VRP and TDR measurements with the TPH analyses of the cores A and B, data from each geophysical method plotted with the core data on a graph (Figures 3-14 and 3-15). Cores data show that the maximum mass of the hydrocarbon appears around a height of 1 m right below the injection well. Both geophysical data and core analyses indicate that the major hydrocarbon concentration exists between a height of about 87 cm and 1.05 cm. Consistent with the geophysical data, the TPH results of core A and B show that there is minor contamination above a height of 1.14 m (the highest point that water level reached after the gasoline spill) within the newly created capillary fringe.

Results from cores A and B show that there are minor gasoline contamination below the lowest water table elevation, which is an artifact of coring; because the part of the cores that were taken from

the saturated zone was holding upright while the piston was taken out. Taking the piston out caused downward movement of the contaminant to the uncontaminated part due to gravity. Comparing TPH results for cores A and B, it can be seen that the concentration of gasoline is much higher in core B, which was taken from the area close to the monitoring well #1 with a thick layer of gasoline. Results from core B show a peak at a height of 1.8 m, which might be an indication of contamination of the top portion of the soil during the gasoline spill.

Feenstra et al. (1991) provided a method to predict the presence of residual NAPL in the soil using the soil chemical analyses. The Feenstra method gives the hypothetical maximum total soil chemical concentration above which the presence of an immiscible phase NAPL is probable. The calculated baseline is shown on Figure 3-15. As can be seen in the figure, there is no residual gasoline up to a height of 0.77 m in core A, nor from a height of 1.23 m to the surface. For core B there is no residual gasoline up to a height of 0.8 m, and between heights of 1.30 m and 1.75 m. For more details about the calculation of maximum total chemical concentration, see Appendix C.

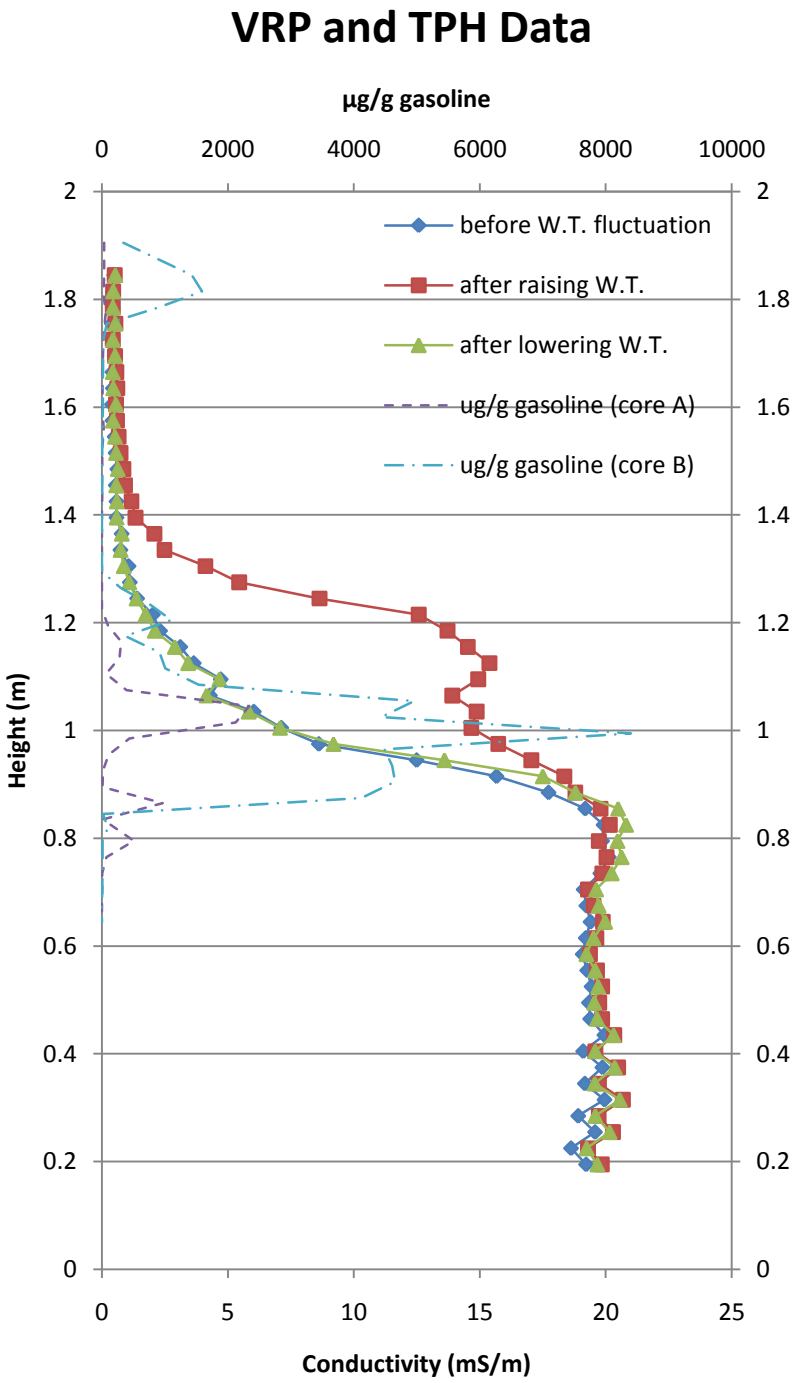

Figure 3-14 Comparison of the core A and B TPH analyses and VRP electrical conductivity profiles; W.T. stands for water table

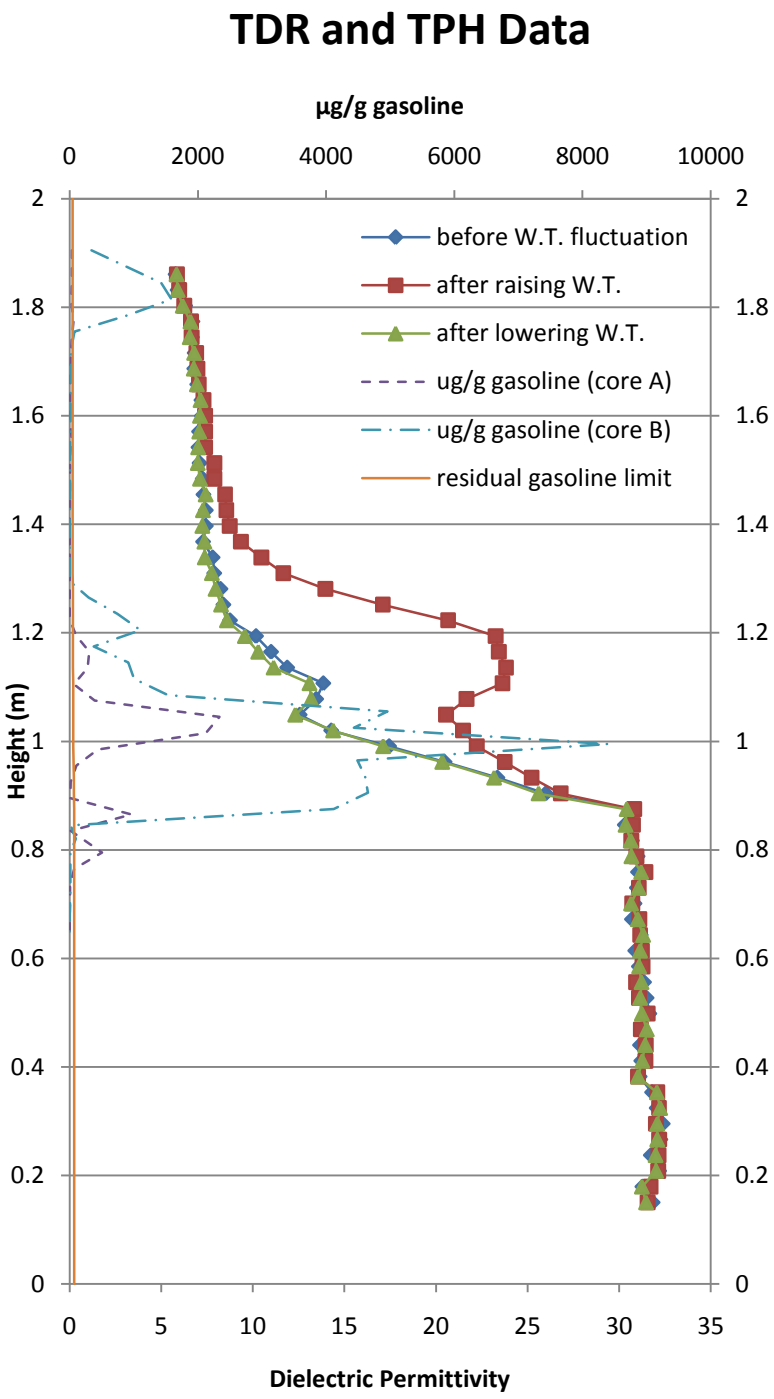

Figure 3-15 Comparison of core A and B TPH analyses and TDR permittivity profiles; W.T. stands for water table

3.4 Water Table Fluctuation 2

To investigate the geophysical responses of smeared gasoline in the saturated zone, the water level was lowered in six different steps during the period between days 110 to 119. In each step, the water level was lowered about 4 to 5 cm. The thickness of the oil layer in the monitoring wells and conductivity and permittivity of the soil were measured before each step. After the last lowering of the water level, the system was allowed to equilibrate for 5 days. At that time, water table was stabilized at a height of 0.46 cm. Subsequently, the water level was raised back to the original level (0.73 m) between days 124 to 132 in four different steps; oil thickness and geophysical measurements were taken before each step. Figures 3-16 shows the electrical conductivity profiles before the water level was lowered and after it was raised back to the original level. Figure 3-17 displays the corresponding permittivity profiles. As can be seen in the figures, the conductivity and permittivity profiles after rising water level back to the original level (imbibition) do not match the profiles measured before the second fluctuation cycle was started (primary drainage), which is related to the pressure-saturation relationship. This hysteresis behavior is due to entrapment of gasoline and/or air during the imbibition. It could have been beneficial to have the geophysically-measured drainage-imbibition curves for the uncontaminated sand and compare them with those from the contaminated sand to find whether the hysteresis is caused by entrapped air or gasoline. However, the change in the slope of the geophysical profiles (after returning the water level to its original level) around a height of about 84 cm, might be an indication of the existence of an entrapped NAPL phase in the previously water saturated zone (i.e., below 87 cm).

Both VRP and TDR measurements indicate that the top of the capillary fringe is at a height of 0.68 m after lowering the water table to a height of 0.46 m (Figures 3-16 and 3-17). Therefore, the capillary fringe thickness decreased by 9 cm compared to that of uncontaminated soil. The length of the capillary fringe after the second cycle of the water table fluctuation is 22 cm, which is larger than that after the third spill (14 cm). The reason could be that the gasoline concentration on top of the capillary fringe is decreased due to smearing during the water table fluctuations.

It can be seen from the Figures 3-16 and 3-17 that the break in the geophysical profiles obtained after lowering the water level 30 cm below the original level disappears, because at this time it is located in the residual saturation zone. Therefore, these two monitoring techniques cannot detect the presence of gasoline in the residual saturated zone, since the electrical conductivity and dielectric

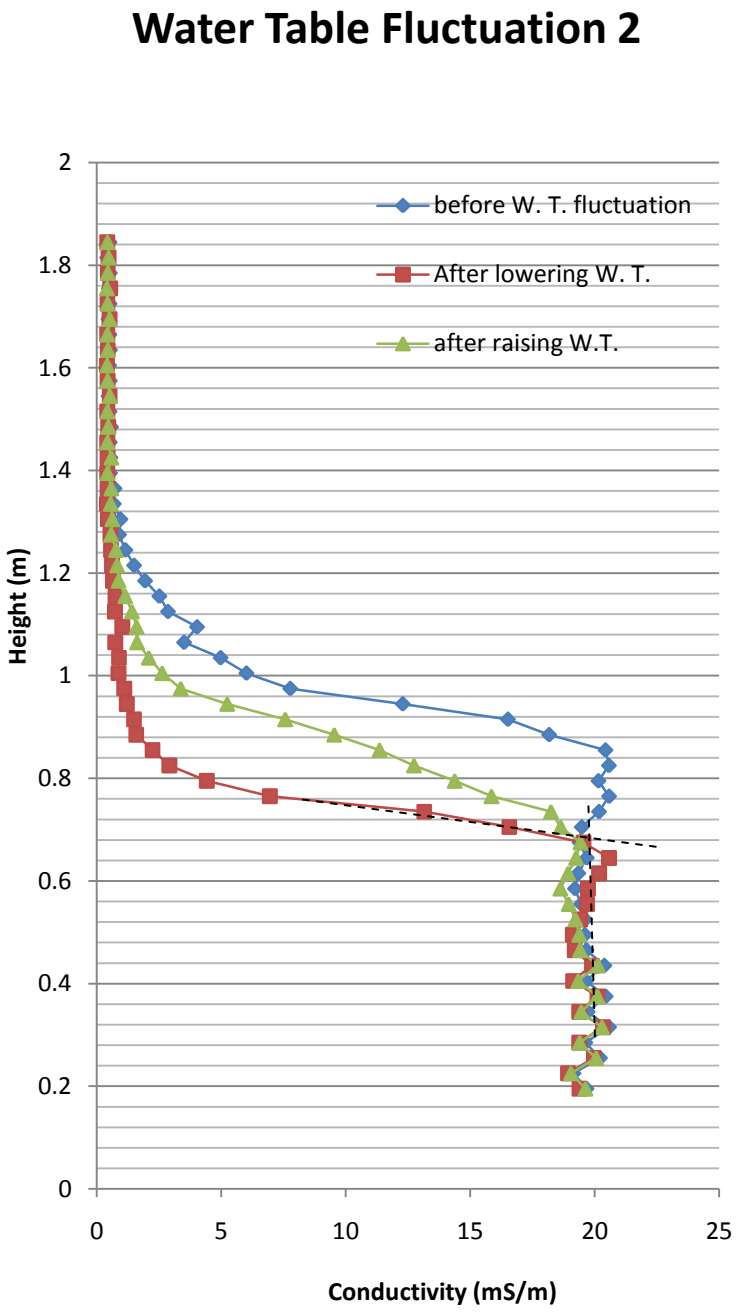

Figure 3-16 Electrical conductivity profiles obtained from VRP measurements during the second water table fluctuation.

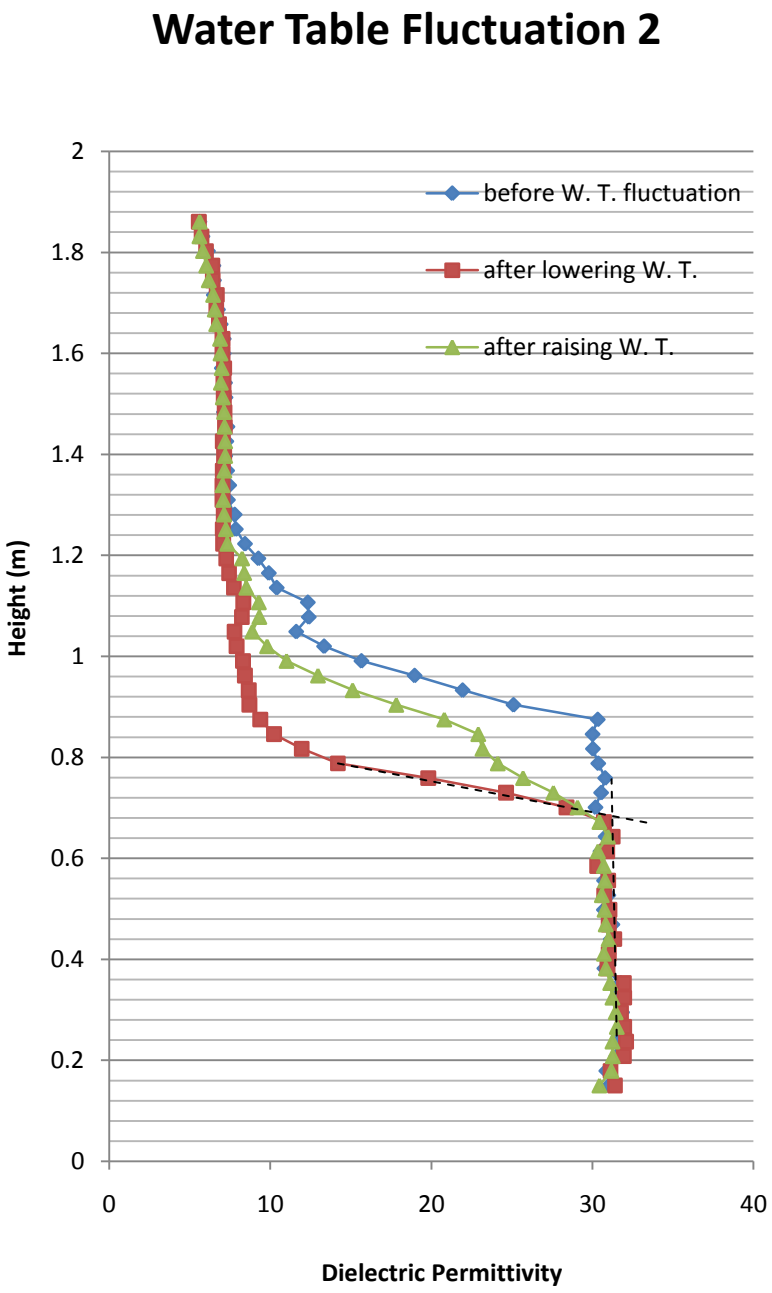

Figure 3-17 Dielectric permittivity profiles obtained from TDR measurements during the second water fluctuation.

permittivity of air and gasoline are similar. However, repeated geophysical measurements with different water table elevations can delineate the presence of contamination fluids.

3.5 Coring 2

After the last step of the second water table fluctuation (on day 132), the system was allowed to reach equilibrium; and cores C and D were taken on day 140. The cores were taken manually using the procedure described in section 3-3. Core C was taken from the area between the TDR rods and the monitoring well #1, and core D was taken from the area between the resistivity electrodes and the monitoring well #2 (Figure 3-13). A total of 47 samples were obtained from each core. Figures 3-18 and 3-19 show the TPH and VRP results; and TPH and TDR results respectively. Again, mass of the gasoline in core C is almost twice the mass in core D. As with core A done during the first cycle, this result appears to reflect the fact that core C was taken from the area close to the monitoring well #1 which had a thick layer of gasoline.

The hydrocarbon profiles (Figures 3-18 and 3-19) show that there is a high amount of gasoline from a height of 68 cm to a height of 88 cm as it was predicted by the geophysical profiles. The TPH result for core D shows a high concentration at a height of 1.8 m similar to the one for core B.

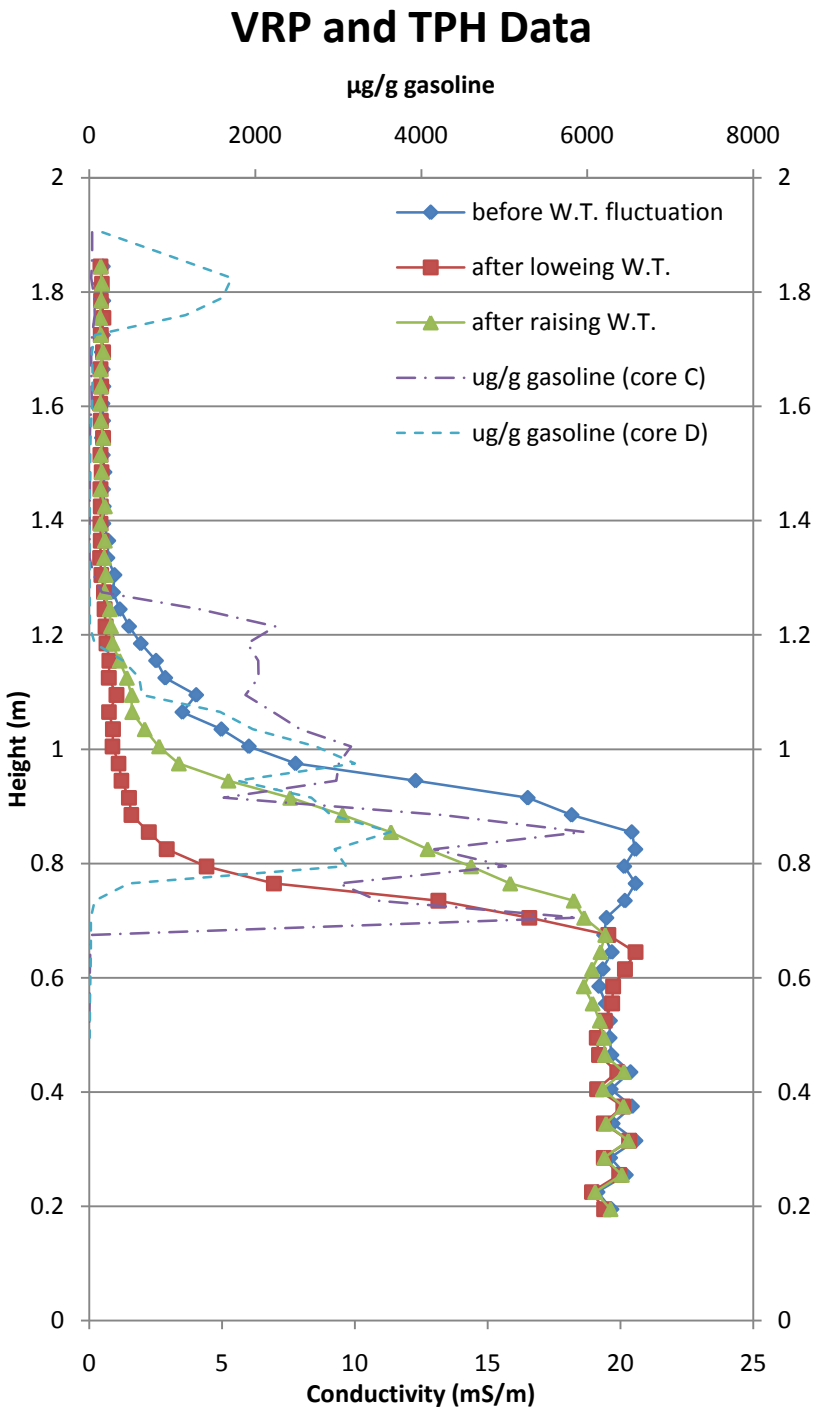

Figure 3-18 Comparison of the VRP and TPH results after lowering the water table 30 cm below the original level.

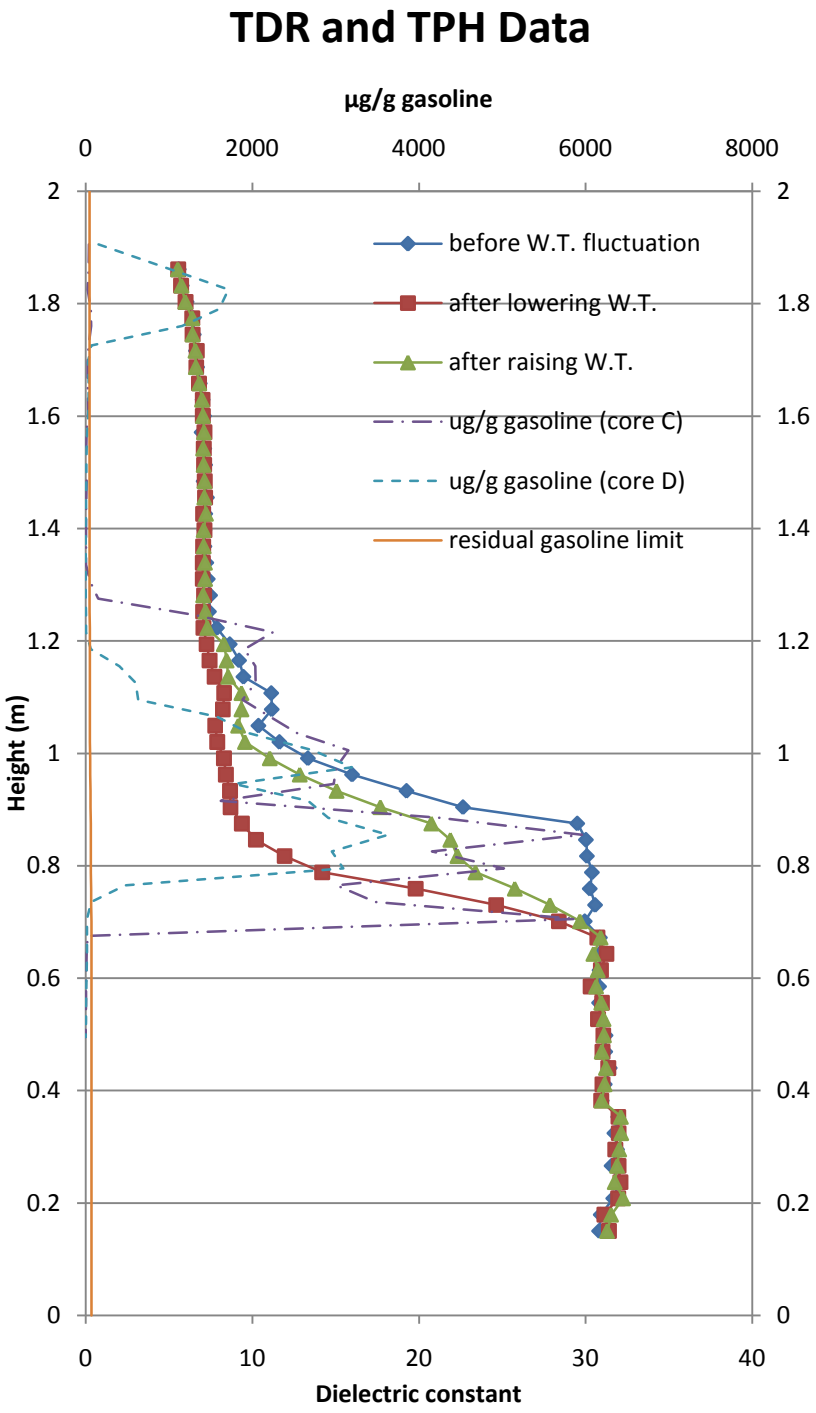

Figure 3-19 Comparison of TDR and TPH results after lowering the water table 30 cm below the original level.

3.6 Comparison of the Electrical Conductivity Profiles Obtained using VRP and TDR Methods

Electrical conductivity is a measure of the ability of a material to conduct charge carriers in response to an applied electrical potential. In general, there are three basic mechanisms for electrical conduction: electronic conduction, electrolytic conduction and interfacial conduction. In clean sand, such as the Borden sand used in this experiment, the primary mechanism is the electrolytic conduction where the charge carriers are ions in the aqueous phase. Hence, the electrical conductivity of the sand is a function of the number of charge carriers available which in turn depends on the ionic concentration, porosity, and water saturation. Further, the electrical conductivity of the sand is the function of the tortuosity of the travel path of the charge carriers in the aqueous phase; this path is determined by pore structure and pore scale fluid distribution of the immiscible fluid phases.

The apparent electrical conductivity of a medium is also a function of the cyclic frequency of the alternating applied potential; this behavior of a physical property is referred as frequency dispersion. In this experiment, we have measurements of apparent conductivity that are obtained at dramatically different frequencies. The TDR method, which is based of electromagnetic wave propagation, operates in the 500 MHz-1GHz frequency range. In contrast, the VRP probe is a galvanic probe that works in the frequency range between 0.5-4 Hz, a factor of 10^{-9} lower that the TDR measurement.

Figure 3-20 displays the electrical conductivity profiles of the column measured by VRP and TDR methods before the gasoline injection. As can be seen in the figure, within the saturated zone, the conductivity values obtained using both methods are nearly identical. In addition, it can be seen that both conductivity profiles exhibit a systematic decrease upward as water saturation decreases. However, the conductivity profiles progressively diverge above the zone of tension saturation and reach their maximum difference occurring in the residual saturation zone.

Gasoline has a very low electrical conductivity; therefore, the conductivity of a medium after contamination by gasoline must be decreased. Figure 3-21 shows the VPR and TDR measured electrical conductivity profiles after the third spill. It can be seen in the figure that when gasoline existed on top of the capillary fringe, the portion of the TDR-measured profile right above the capillary fringe matches with the same portion of the VRP-measured profile. Therefore, presence of LNAPL affects the electrical conductivity values measured by TDR method. To examine the effect of gasoline on VRP and TDR measured electrical conductivity, the conductivity profiles obtained before and after each spill are plotted on Figures 3-22 and 3-23. Both figures show that gasoline decreased

the electrical conductivity of the medium; however, the conductivity variations are large with the VRP method.

Additional plots of TDR and VRP-measured conductivity profiles during the water table fluctuations are found in Appendix D.

Persson and Berndtsson (2002) have done calibration experiments in homogenous sand using different LNAPLs. They mixed a known amount of water, LNAPL and soil and measured dielectric permittivity and electrical conductivity of the soil using TDR method. They concluded that LNAPL content has a larger effect on the electrical conductivity than the dielectric permittivity of the medium. Haridy et al. (2004) have done a similar experiment on fine sand samples and concluded that the presence of LNAPLs in the medium increased the apparent dielectric permittivity but had no significant effect on the apparent conductivity. Nevertheless, their experiment is not representative of either my experiment or actual LNAPL contamination.

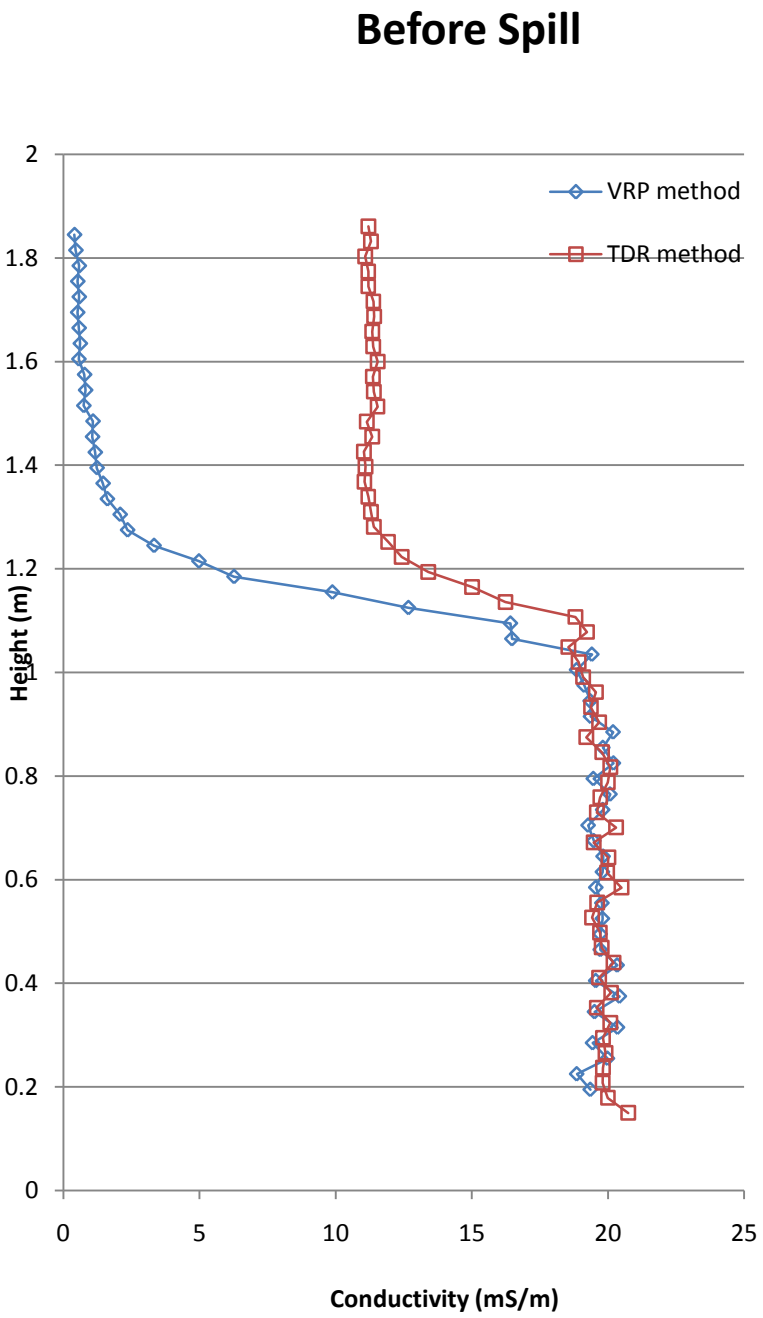

Figure 3-20 Electrical conductivity profiles obtained using TDR and VRP methods before the spill

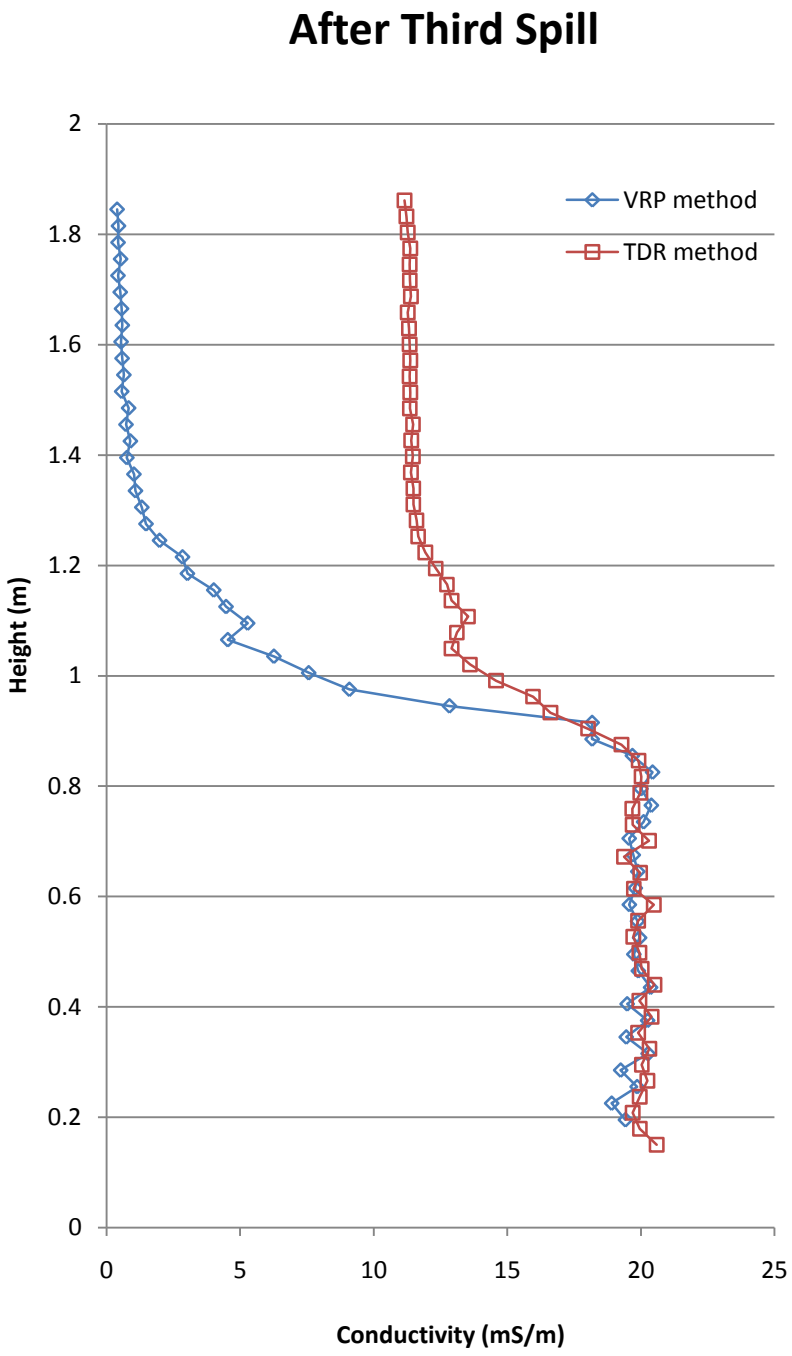

Figure 3-21 Electrical conductivity profiles obtained using TDR and VRP methods after the third spill

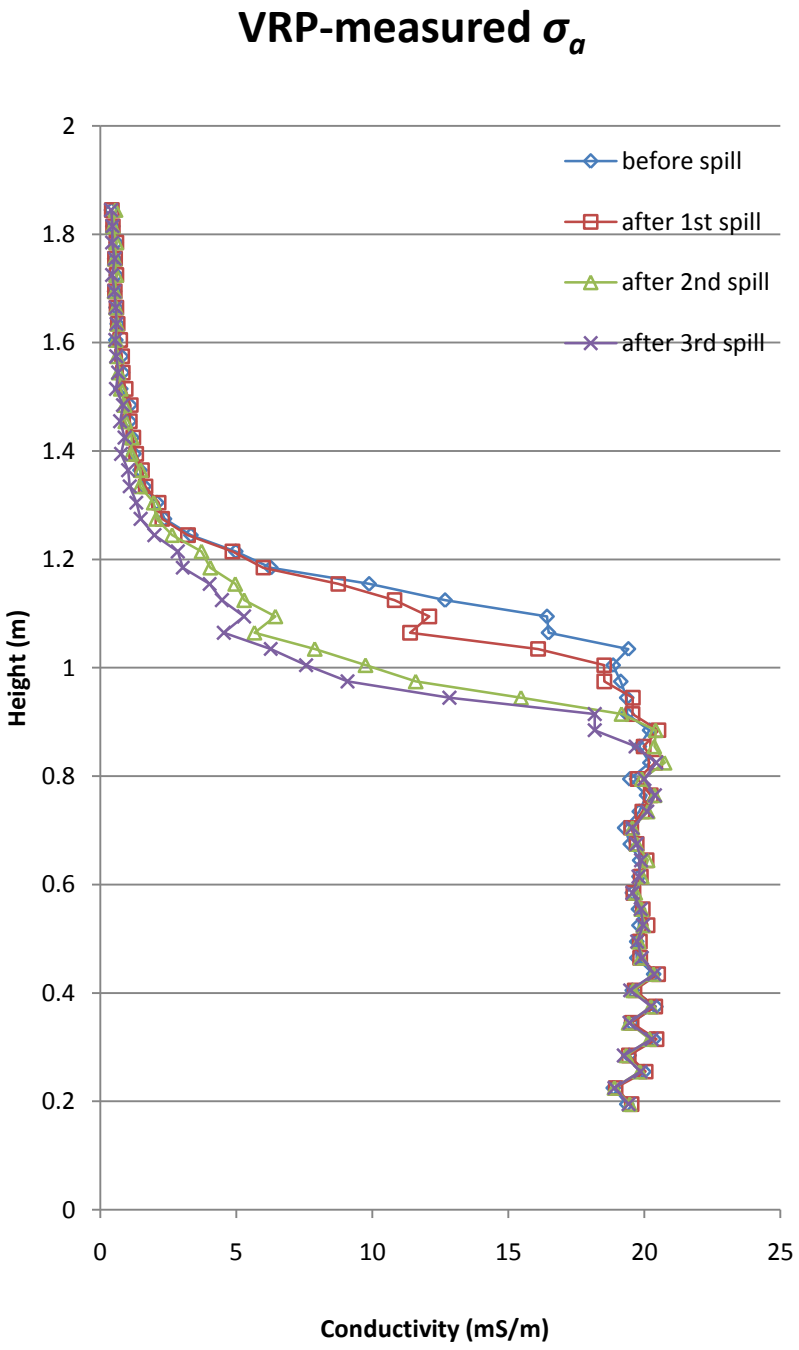

Figure 3-22 Change in the electrical conductivity profiles obtained from VRP measurements before and after each spill

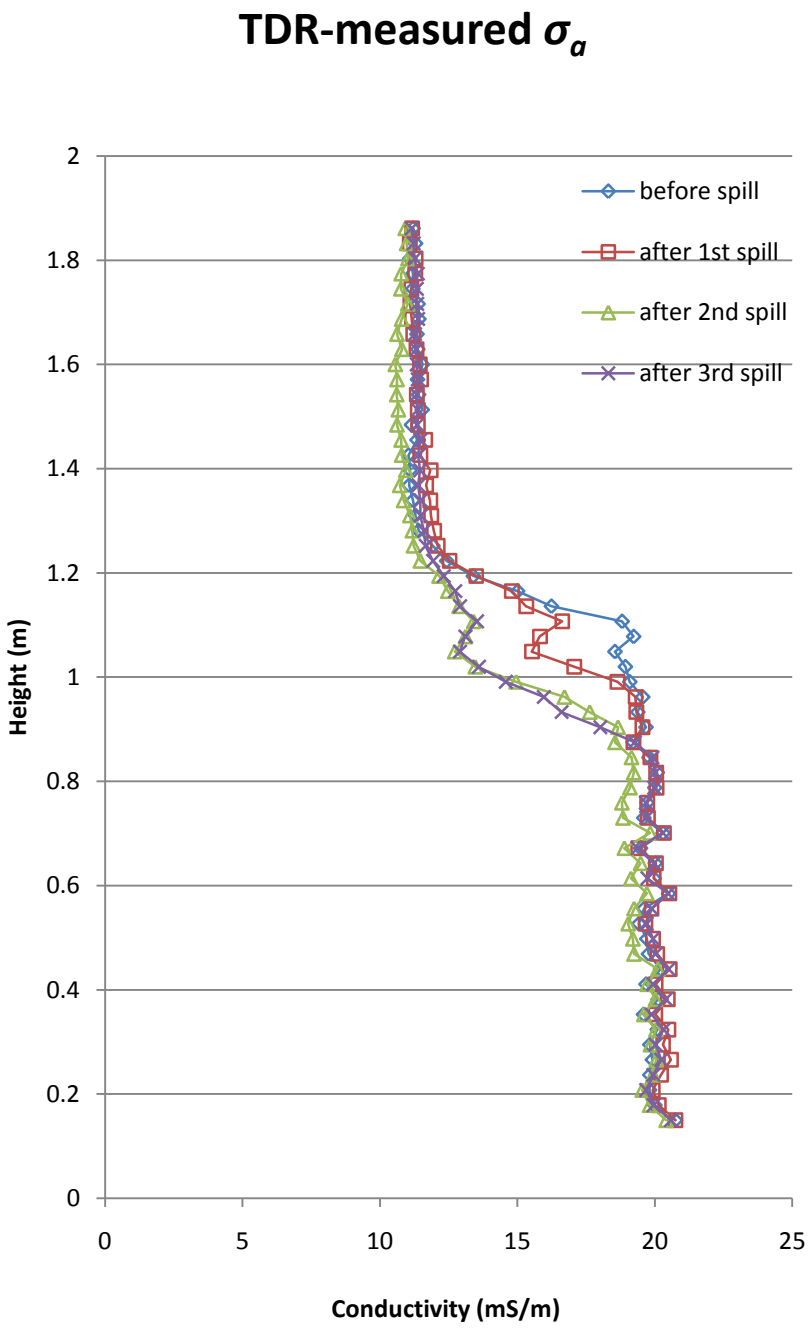

Figure 3-23 Change in the dielectric permittivity profiles obtained from TDR measurements before and after each spill

Chapter 4
Calculation of Water Saturation

In the previous chapter, the relative changes obtained using TDR and VRP methods before and after the spill, and during the water table fluctuation was discussed. In this chapter, we will examine the estimation of water saturation (S_w) based on the geophysical data, using perophysical relationships proposed in the literatures.

4.1 Pre-release Geophysical Data

4.1.1 Calculation of S_w from Conductivity Data

One well-known relationship between the conductivity and water content of the soil is Archie's empirical law (equation 2-13). Many scientists have investigated Archie's law and found that *a*, *m*, and *n* are specific for each material. In his paper, Archie states that the value *a*=1 and *m* ~1.3 are reasonable for clean unconsolidated sand while *m* varies between 1.8 and 2 for consolidated sandstones. Bussian (1983) also argues that *a* should be equal to 1 for unconsolidated sand, while Winsauer et al. (1952) showed that *a*=0.62 give the best fit to their data. Hence, the form of the Archie's equation in which *a* takes values other than 1 sometimes is called Winsauer equation (Ward and Fraser, 1967). Data from Sen et al. (1981), Johnson et al. (1982), Schwartz et al. (1989), and Revil and Cathles (1999) show that the cementation factor (*m*) for glass beads and sand lies between 1.5 to 2. Pape et al. (1987) found that *m* ranges from 1.5 to 2 for clean and slightly shaly sandstones. To avoid the uncertainty of *a* and *m* values, in this work, equation 2-15 was used to calculate the water saturation from conductivity data.

$$S_w = \left(\frac{\sigma_a}{\sigma_{sat.}} \right)^{\frac{1}{n}} \qquad 4\text{-}1$$

Use of this normalized quantity requires only the determination of the saturation exponent *n*. The saturation exponent *n* is commonly set to 2 for different materials including clean unconsolidated sand and glacial aquifer (Archie, 1942; Frohlich and Parke, 1988; Telford et al., 1990). However, Gorman and Kelly (1989) showed that *n* is close to 1.5 for Ottawa sand.

Mickle (2005) found that the water saturation profile of the packed Borden sand obtained using *n*=1.6 gives the best match to the profile obtained using van Genuchten hydrogeological model at

residual saturation. The water saturation profiles obtained using *n*=1.5 and *n*=2 from the pre-release conductivity data are shown in Figure 4-1. In the case of *n*=1.5, the residual water saturation is around 0.08, which gives the residual water content value of about 0.03 if it is normalized by the measured porosity of the packed Borden sand (0.41). However, *n*=2 gives the residual water saturation value of about 0.17, which is equal to residual water content value of about 0.07, which is consistent with the value measured in the laboratory by Nwankwor (1982). Therefore, the saturation exponent *n*=2 is reasonable for the packed Borden in this study. The saturation profile obtained using *n*=2 will be compared with the saturation profiles obtained using TDR measurements.

4.1.2 Calculation of S_w from TDR Data

The most commonly used equation for calculation of water content from dielectric permittivity is Topp's equation for all mineral soil:

$$\theta = -5.3 \times 10^{-2} + 2.92 \times 10^{-2}\kappa_a - 5.5 \times 10^{-4}\kappa_a^2 + 4.3 \times 10^{-6}\kappa_a^3 \qquad 4\text{-}2$$

In Figure 4-2, the water saturation profile obtained from the pre-release TDR data using Topp's general equation is compared to that of obtained from conductivity data using Archie's equation with *n*=2. It should be noted that the water content calculated using Topp's equation is normalized to the TDR derived water content of the saturated zone in order to express the results in terms of the water saturation. As can be seen in the figure, Topp's equation overestimates the water saturation in the unsaturated zone.

Since Borden sand is clean, it was felt that the relationships for glass beads obtained by Topp et al. (1980) could give a better match to the VRP results. Topp et al. (1980) provided the relationships for calculation of the permittivity values from the water content values for glass beads of 30 μm, 450 μm, and a 30 μm-450 μm mixture, while we want to measure the water content from the measured permittivity; hence, the inverse relationships for glass beads was found (see Appendix E for the original and inverse equations plots) and the resulted water saturation profiles was compared to that of obtained using Archie's equation (Figure 4-3). The best match between the TDR and VRP results was obtained with the Topp's relationship for 30 μm glass beads:

$$\theta = -7.96 \times 10^{-2} + 2.33 \times 10^{-2}\kappa_a - 3.11 \times 10^{-4}\kappa_a^2 + 2.81 \times 10^{-6}\kappa_a^3 \qquad 4\text{-}3$$

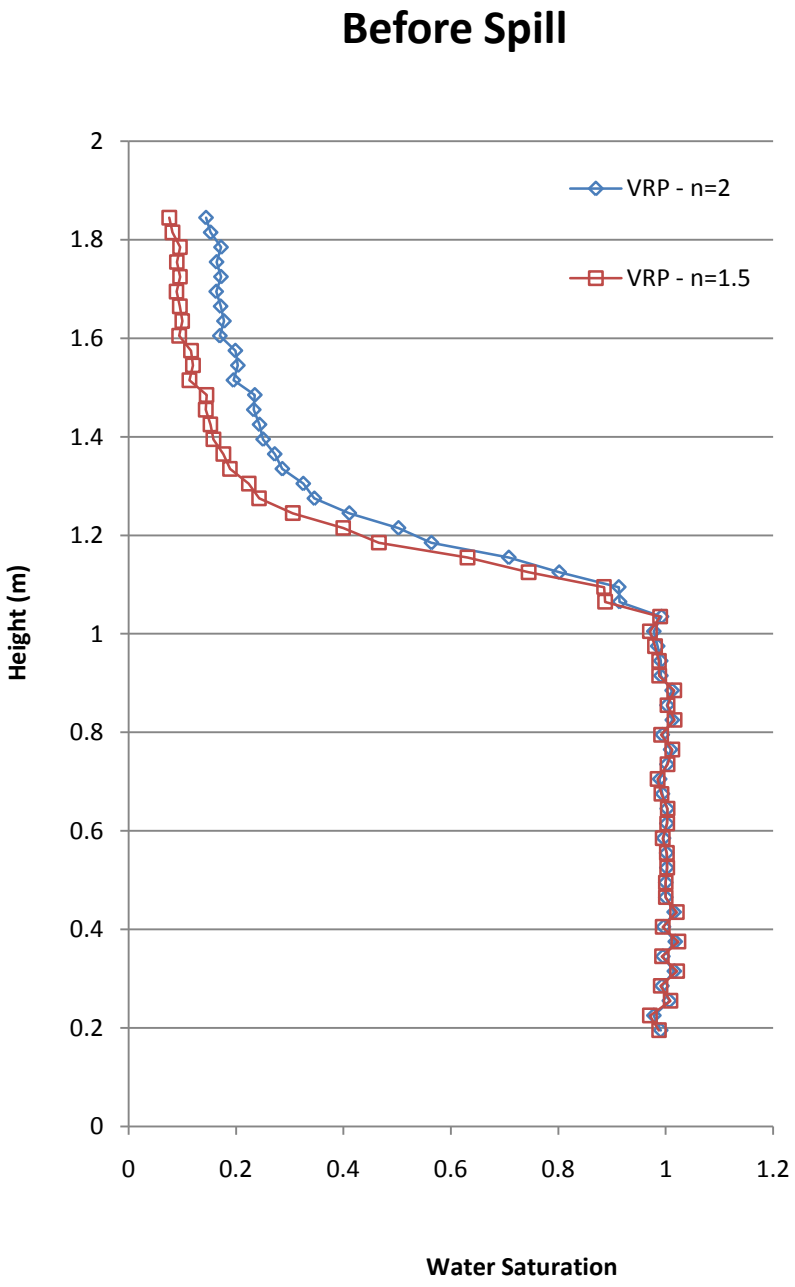

Figure 4-1 Water saturation profiles calculated from conductivity data. Archie's equation with *n*=1.5 and *n*=2 was used to convert the conductivity data to water saturation values.

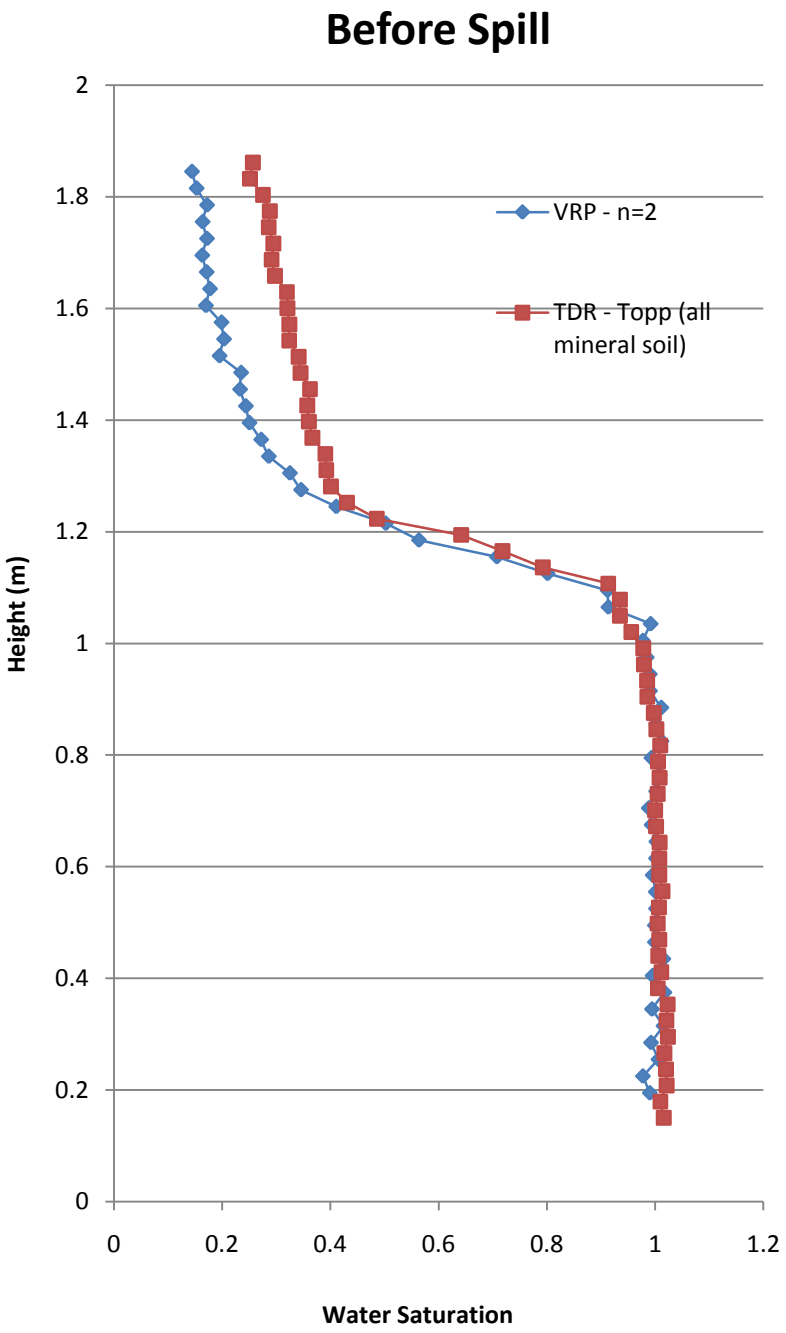

Figure 4-2 Comparison of the water saturation profiles obtained from VRP conductivity data using Archie's equation with *n*=2, and from TDR data using standard Topp's equation

Porosity is the measure of the voids between the solid particles of a material. In the saturation zone, where all of the pores are filled with water, porosity is equal to the water content. Topp's equation for all mineral soil gives the water content values of around 0.45 for the saturated part of the column (and therefore a porosity of 0.45); while Topp's equation for 30 µm glass beads gives the values of around 0.42. Porosity of the packed sand column was measured to be 0.41 using the bulk dry density of a core sample from the column, further indicating that the 30 µm glass beads relationship gives more accurate water content values in the experimental column.

Figure 4-4 displays the comparison of the Topp's equation for 30 µm glass beads to the equations developed by Jacobsen and Schjønning (1993), and Ferré et al. (1996); and the mixing model (see section 2.1.1). In the mixing model, κ_w, κ_s, and κ_{air} were given the values of 78.16 (at 25˚C and 1GHz), 4.42, and 1 respectively (Handbook of Chemistry and Physics, 88th Edition, 2007-2008), and ϕ was assumed to be 0.41 to calculate the water content. Then the water content values were normalized to the water content of the saturated zone, which was 0.61, to obtain water saturation values.

Compared to the Topp's equation for 30 µm glass beads, all of the other equations discussed above, overestimate the water content. Therefore, the preferred equation to calculate water content from dielectric permittivity for uncontaminated Borden sand is the Topp's equation for 30 µm glass beads.

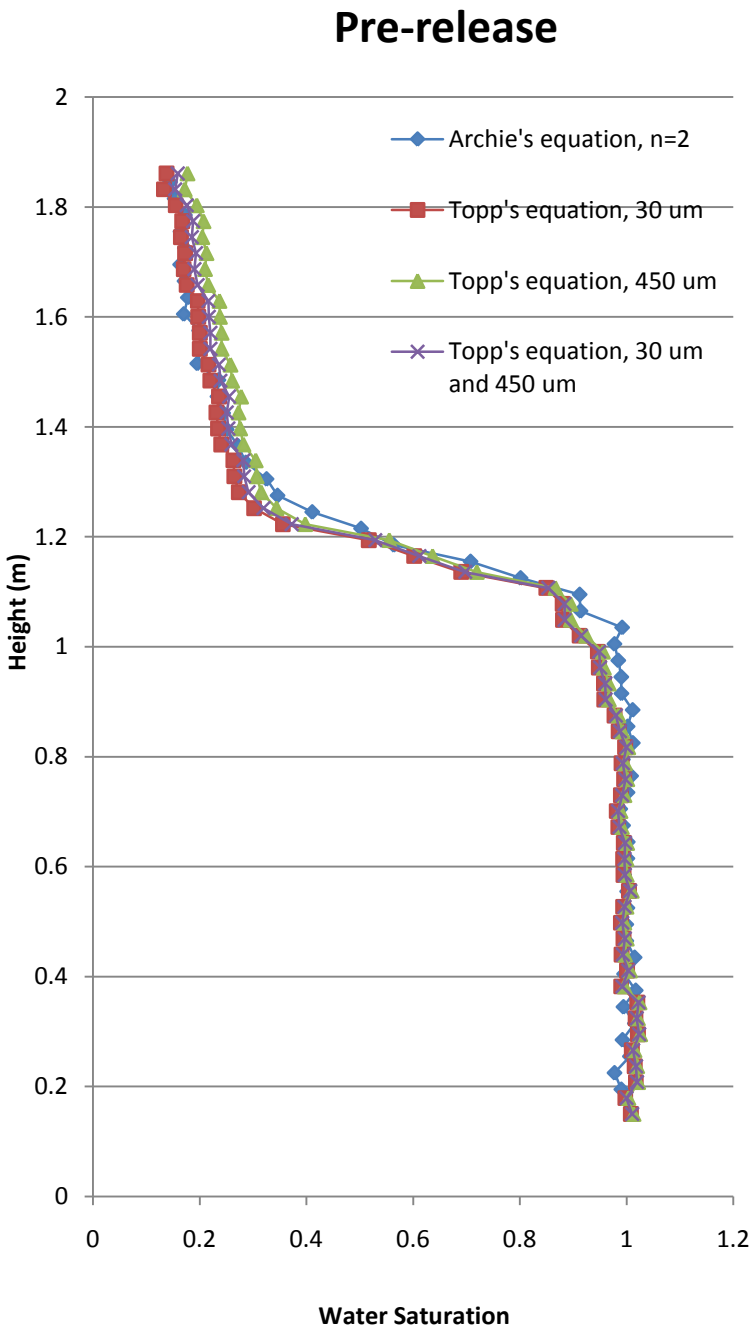

Figure 4-3 Comparison of the water saturation profiles obtained from conductivity data using Archie's equation with *n*=2 and from TDR data using Topp's equation for glass beads of different sizes

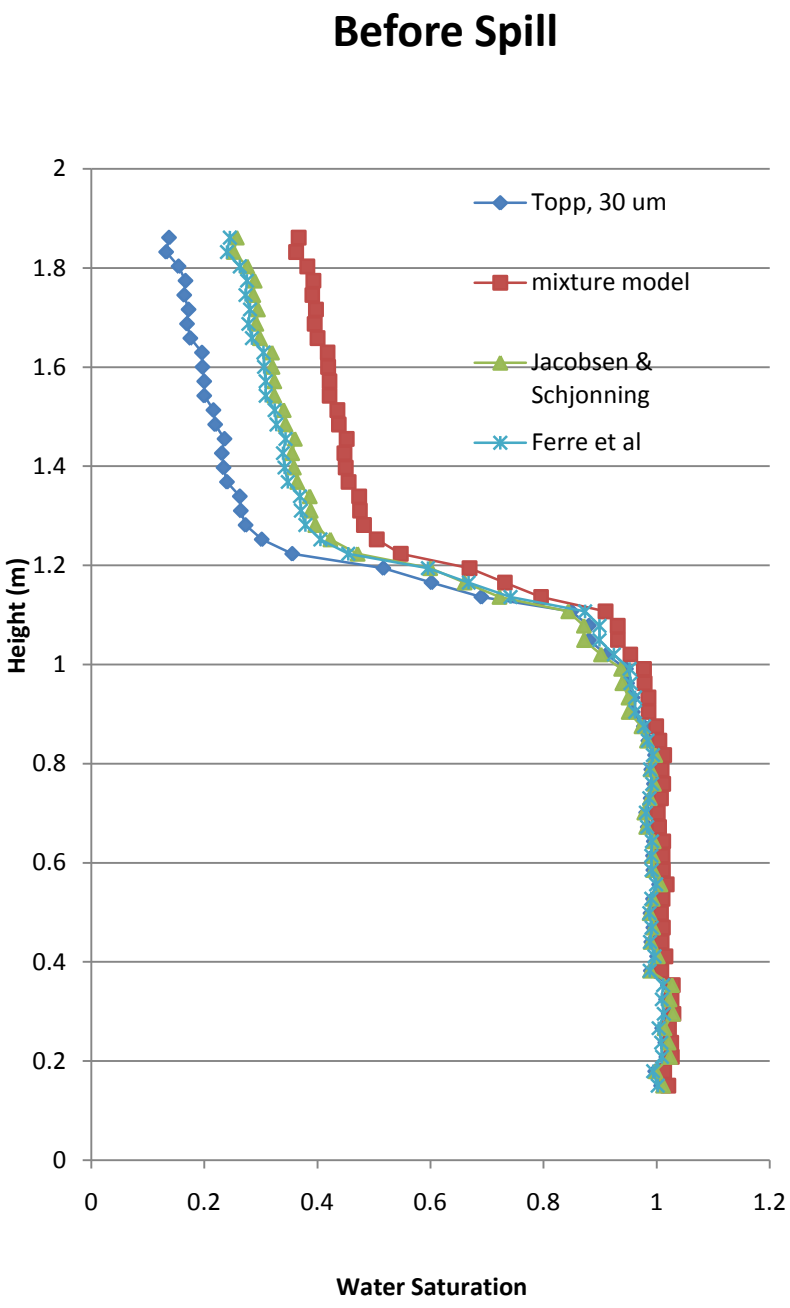

Figure 4-4 Comparison of the water saturation profiles obtained using different equations before the gasoline spill

4.2 Post-release Geophysical Data

The total amount of 3.36 liters of gasoline was injected into the column in three steps and measurements were taken after each injection. As discussed in chapter 3, the maximum change in the conductivity and dielectric permittivity profiles happened after the second injection. Therefore, geophysical data after the second injection will be used to compare the resulting water saturation profiles.

In section 4.1.1, it was found that n=2 yields the best water saturation values for the uncontaminated Borden sand in the column. In addition, Topp's equation for 30 µm glass beads is the best equation to convert TDR measured apparent dielectric permittivity to water saturation. Both Archie's law and Topp's equation were developed for three-phase systems (air-water-soil). However, one could reasonably expect that those equations may not work after adding gasoline to the system.

Figure 4-5 displays a comparison of the water saturation profiles obtained using TDR permittivity and VRP conductivity data after the spill. It can be seen that the water saturation profiles diverge in the transition zone where the gasoline resides. Hence, it is apparent that other relationships are needed for characterization of the four-phase system (water-NAPL-air-solid) that exists after contamination.

Persson and Berndtsson (2002) proposed an equation to calculate θ_w from TDR measured κ_a and σ_a of a four-phase system:

$$\theta_w = 0.0338\kappa_a + 0.0002\kappa_a^2 + 0.1523\sigma_a + 1.2888\sigma_a^2 - 0.0701\kappa_a\sigma_a - 0.093 \qquad 4\text{-}4$$

This equation was applied to the data after the third spill and the resulted water content profile was compared to that of obtained using Topp's equation for 30 µm glass bead (Figure 4-6). As can be seen in the figure, the equation overestimates the water content by a factor of 2. However, if the water content values are normalized with the water content of the saturated zone, the resulted water saturation profile is very close to the one obtained using Topp's equation for 30 µm glass beads (Figure 4-7). Persson and Berndtsson (2002) also showed an approach to find the volumetric LNAPL content (θLNAPL) of the unsaturated zone using κ_a and σ_a. However, as discussed in section 3-6, their approach cannot be used for the actual LNAPL contamination.

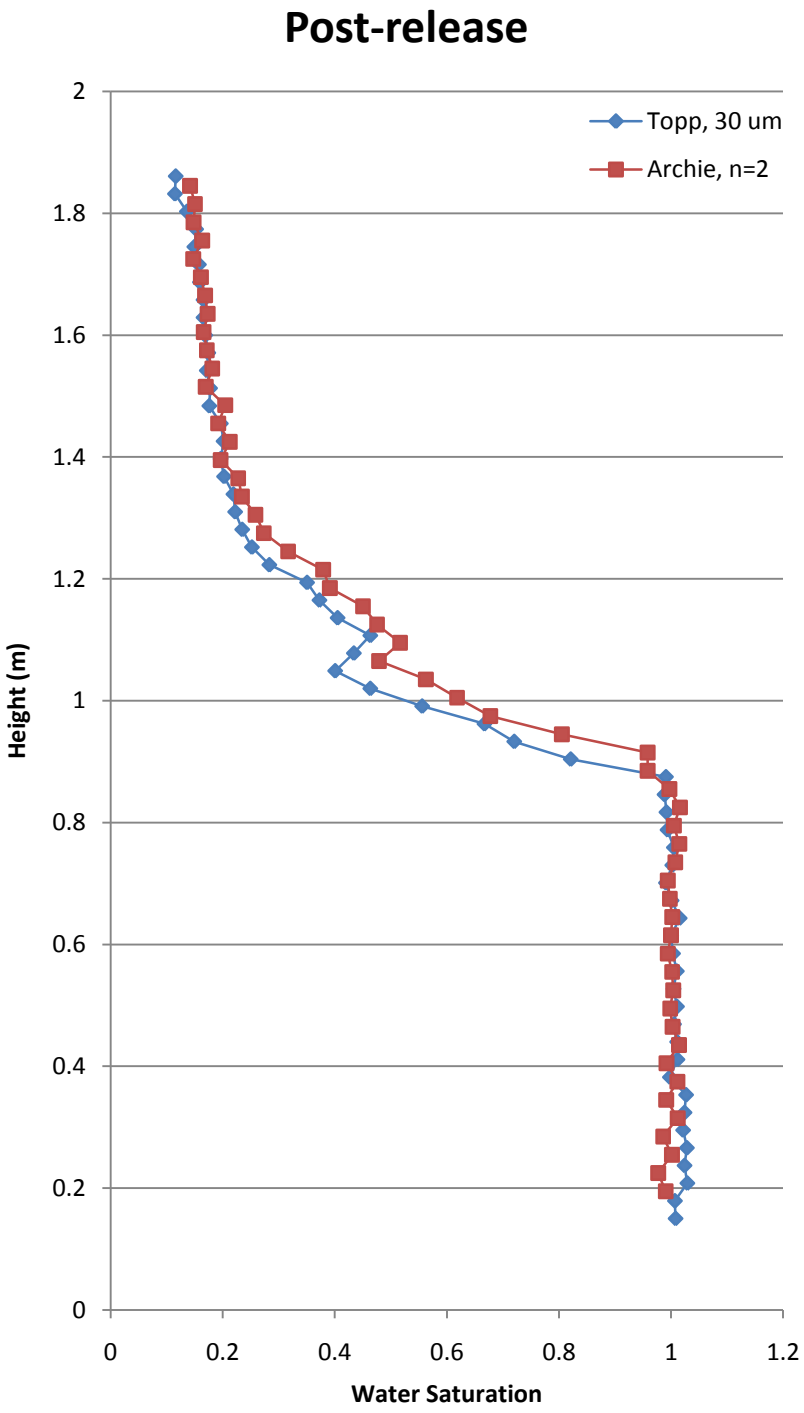

Figure 4-5 Comparison of the water saturation profiles obtained using TDR and conductivity data after the third spill

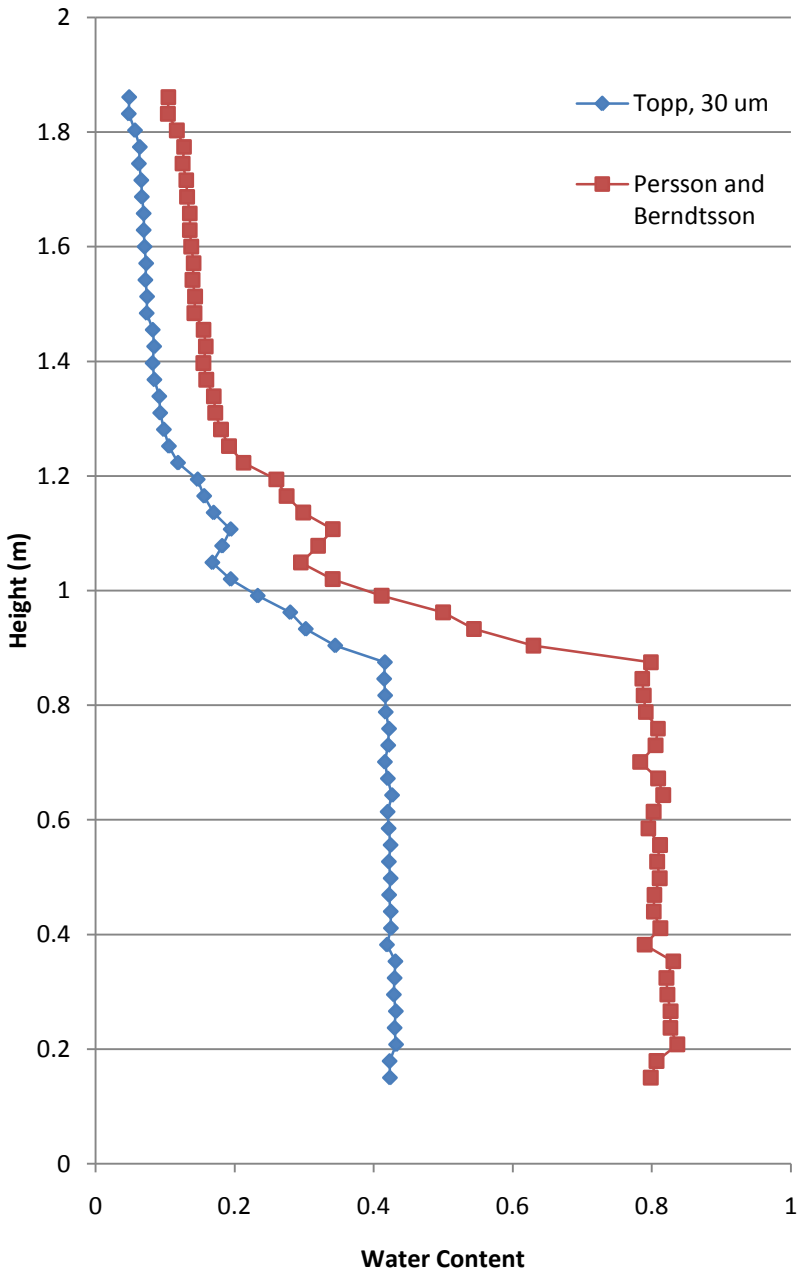

Figure 4-6 Comparison of the water content profiles obtained using the equation provided by Persson and Berndtsson (2002) and Topp's equation for 30 µm glass beads (1980).

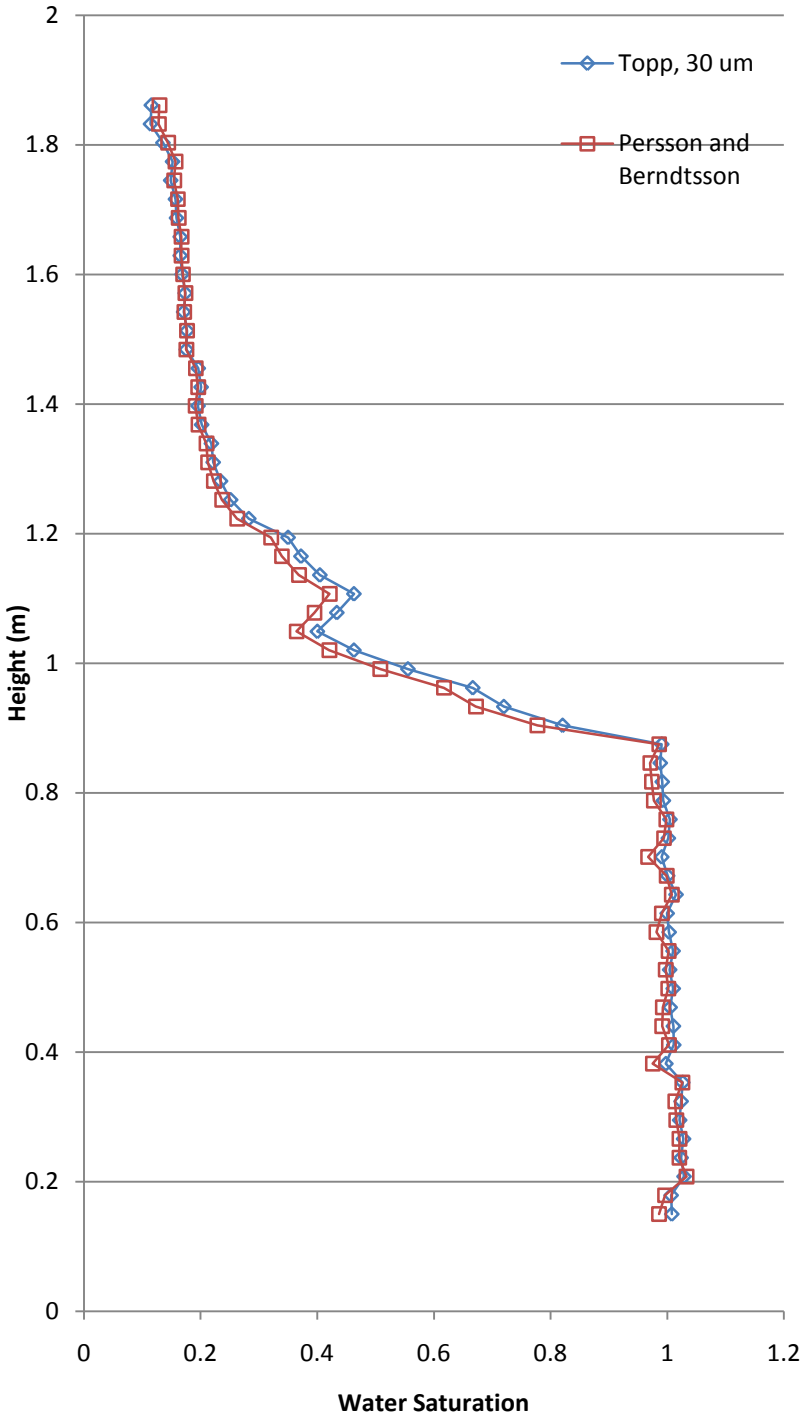

Figure 4-7 Comparison of the water saturation profiles obtained using the equation provided by Persson and Berndtsson (2002) and Topp's equation for 30 µm glass beads (1980).

Chapter 5
Conclusions and Recommendations

The large scale of the column facilitated the creation of the vadose and saturated zones similar to field conditions and gave us the opportunity of using two different geophysical techniques. The high resolution and controlled nature of the experiment enabled the detailed monitoring of geophysical response to introduction of gasoline and the subsequent water table fluctuations. Both VRP and TDR methods showed a measurable response to a small amount of gasoline injected during the first spill. The gasoline injection was happened close to the tension saturation zone and desaturation of the pores appeared as a break on the electrical conductivity and permittivity profiles. The break had a lower conductivity and permittivity values and expanded as more gasoline was added to the system.

The 31 cm capillary fringe thickness of the uncontaminated Borden sand used for this experiment was reduced to 22 cm after first injection of 1 liter of gasoline. The volume of effluent water from the system after the first injection was 3 times the injected gasoline volume. Clearly, the presence of gasoline reduced the surface tension, resulting in a large amount of water being released from the system and the reduction of the capillary fringe thickness. After addition of a further 2 liters of gasoline during the second injection, the capillary fringe thickness was reduced a further 8 cm and the effluent water was about two times the volume of the injected gasoline. The capillary fringe thickness did not changed after release of additional 2 liters of gasoline during the third injection and the volume of the effluent water was the same as the volume of the injected gasoline, which might be an indication that the capillary fringe thickness could not be decreased further due to the establishment of a preferential LNAPL flow path to one of the wells.

The geophysical response of the water table fluctuation in the presence of gasoline was monitored in this experiment. The electrical conductivity and permittivity profiles after the water table was established above the original level clearly showed the presence of entrapped gasoline below the newly established water table. However, these two geophysical techniques are not able to detect gasoline in the residual water saturation zone where pores are mostly filed with air and gasoline, because the electrical conductivity and permittivity of gasoline and air are similar. Since these two methods are able to show the entrapped gasoline nearby or below the water table, repeated geophysical measurements over time with different water table elevations can delineate the location of the immiscible contaminant phase in the subsurface. The electrical conductivity and permittivity

profiles after the water level was raised back to its original level did not match the profiles obtained before the cycle was started, which is an indication of entrapped gasoline below the water table.

TDR method measures dielectric permittivity and electrical conductivity of a medium simultaneously from the propagation of a high-frequency electromagnetic wave through the soil. The VRP method applies a DC current into the soil and calculated the conductivity from the measured potential. The electrical conductivity profiles obtained from TDR method match the profiles obtained from VRP method in the saturated zone; however, the TDR measured conductivity values are higher than those measured by VRP method in the unsaturated zone. The frequency-dependant nature of the electrical conductivity is an interesting issue, which needs further investigation.

The VRP measured electrical conductivity values can be converted to the water saturation values using Archie's empirical law. The saturation component *n* for the uncontaminated Borden sand used in this experiment was found to be equal to 2. Topp's equation for all mineral soil has been used commonly to convert the TDR measured dielectric permittivity. However, Topp's equation for all mineral soil overestimates the water saturation for uncontaminated Borden sand when it is compared to the water saturation calculated using Archie's law with n=2. The best fit to the water saturation profile obtained from the VRP measurements was found to be the profile obtained using Topp's equation for 30 µm glass beads. The water saturation profiles obtained from Archie's law and Topp's equation for 30 µm glass beads diverged when gasoline was introduced to the system. Several researchers have performed calibration experiments in a four phase system (water-air-LNAPL-soil) to find the relationship between the dielectric permittivity and fluid content of a medium; but their approach needs in-depth investigation.

For further study related to this experiment, the pre-release and post-release water saturation profiles obtained using the petrophysical relationships can be compared to the hydrological models such as van Genuchten and Brooks-Corey models.

Remediation of the column using ethanol injection and monitoring of the geophysical response to the remediation process is recommended. This would provide information about the usefulness of the VRP and TDR techniques for remediation purposes.

References

CRC handbook of chemistry and physics : A ready-reference book of chemical and physical data. 2007 - 2008.

Archie, G. E. 1942. The electrical resistivity log as an aid in determining some reservoir characteristics. *Transactions of the American Institute of Mining and Metallurgical Engineers* 146, : 54-61.

Bevan, M. J., A. L. Endres, D. L. Rudolph, and G. Parkin. 2005. A field scale study of pumping-induced drainage and recovery in an unconfined aquifer. *Journal of Hydrology* 315, (1-4) (DEC 10): 52-70.

Birchak, J. R., C. G. Gardner, J. E. Hipp, and J. M. Victor. 1974. High dielectric-constant microwave probes for sensing soil-moisture. *Proceedings of the IEEE* 62, (1): 93-8.

Bussian, A. E. 1983. Electrical conductance in a porous-medium. *Geophysics* 48, (9): 1258-68.

Dasberg, S., and J. W. Hopmans. 1992. Time domain reflectometry calibration for uniformly and nonuniformly wetted sandy and clayey loam soils. *Soil Science Society of America Journal* 56, (5) (SEP-OCT): 1341-5.

Davis, J. L., and W. J. Chudobiak. 1975. In situ meter for measuring relative permittivity of soils; report of activities, april to october 1974, geophysics. *Paper - Geological Survey of Canada* 75-1, (75-1): 75-80.

Drungil, C. E. C., K. Abt, and T. J. Gish. 1989. Soil-moisture determination in gravelly soils with time domain reflectometry. *Transactions of the ASAE* 32, (1) (JAN-FEB): 177-80.

Fellner-Feldegg, Hugo. 1972. A thin-sample method for measurement of permiability, permittivity, and conductivity in the frequency and time domain. *J. Phys. Chem.* 76, : 2116-2122.

———. 1969. Measurement of dielectrics in the time domain. *Journal of Physical Chemistry* 73, (3): 616-23.

Ferre, P. A., D. L. Rudolph, and R. G. Kachanoski. 1996. Spatial averaging of water content by time domain reflectometry: Implications for twin rod probes with and without dielectric coatings. *Water Resources Research* 32, (2) (FEB): 271-9.

Frohlich, R. K., and C. D. Parke. 1989. The electrical resistivity of the vadose zone — field Survey . 27, (4): 524-530.

Gorman, T., and W. E. Kelly. 1990. Electrical hydraulic-properties of unsaturated ottawa sands. *Journal of Hydrology* 118, (1-4) (OCT): 1-18.

Grantz, D. A., M. H. Perry, and F. C. Menizer. 1990. Using time-domain reflectometry to measure soil water in hawaiian sugarcane. *Agronomy Journal* 82, : 144-146.

Haridy, Sahar Ahmed, Magnus Persson, and Ronny Berndtsson. 2004. Estimation of LNAPL saturation in fine sand using time-domain reflectometry. *Hydrological Sciences Journal = Journal Des Sciences Hydrologiques* 49, (6) (Dec): 987-1000.

Heimovaara, T. J. 1993. Design of triple-wire time-domain reflectometry probes in practice and theory. *Soil Science Society of America Journal* 57, (6) (NOV-DEC): 1410-7.

Jacobsen, O. H., and P. Schjonning. 1993. A laboratory calibration of time-domain reflectometry for soil-water measurement including effects of bulk-density and texture. *Journal of Hydrology* 151, (2-4) (NOV): 147-57.

Knight, J. H. 1992. Sensitivity of time domain reflectometry measurements to lateral variations in soil-water content. *Water Resources Research* 28, (9) (SEP): 2345-52.

Ledieu, J., P. Deridder, P. Declerck, and S. Dautrebande. 1986. A method of measuring soil-moisture by time-domain reflectometry. *Journal of Hydrology* 88, (3-4) (NOV 30): 319-28.

Mickle, Robert James. 2005. *Coupled hydrogeological-petrophysical analysis of geophysical variation in the vadose zone*. Waterloo, Ont.: University of Waterloo.

Nwankwor, G. I. 1982. A comparative study of specific yield in a shallow unconfined aquifer.University of Waterloo.

Pape, H., L. Riepe, and J. R. Schopper. 1987. Interlayer conductivity of rocks - a fractal model of interface irregularities for calculating interlayer conductivity of natural porous mineral systems. *Colloids and Surfaces* 27, (1-3) (OCT): 97-122.

Patterson, D. E., and M. W. Smith. 1985. Unfrozen water-content in saline soils - results using time-domain reflectometry. *Canadian Geotechnical Journal* 22, (1): 95-101.

———. 1981. The measurement of unfrozen water-content by time domain reflectometry - results from laboratory tests. *Canadian Geotechnical Journal* 18, (1): 131-44.

———. 1980. The use of time domain reflectometry for the measurement of unfrozen water-content in frozen soils. *Cold Regions Science and Technology* 3, (2-3): 205-10.

Persson, M., and R. Berndtsson. 2002. Measuring nonaqueous phase liquid saturation in soil using time domain reflectometry. *Water Resources Research* 38, (5) (MAY): 1064.

Reeves, T. L., and S. M. Elgezawi. 1992. Time domain reflectometry for measuring volumetric water-content in processed oil-shale waste. *Water Resources Research* 28, (3) (MAR): 769-76.

Revil, A., and L. M. Cathles. 1999. Permeability of shaly sands. *Water Resources Research* 35, (3) (MAR): 651-62.

Reynolds, John M. 1997. *Introduction to applied and environmental geophysics*. Chichester ; New York: John Wiley.

Roth, C. H., M. A. Malicki, and R. Plagge. 1993. Empirical-evaluation of the relationship between soil dielectric-constant and volumetric water-content as the basis for calibrating soil-moisture measurements by tdr (vol 43, pg 1, 1992). *Journal of Soil Science* 44, (4) (DEC): 749-.

———. 1992. Empirical-evaluation of the relationship between soil dielectric-constant and volumetric water-content as the basis for calibrating soil-moisture measurements by tdr. *Journal of Soil Science* 43, (1) (MAR): 1-13.

Roth, K., R. Schulin, H. Fluhler, and W. Attinger. 1990. Calibration of time domain reflectometry for water-content measurement using a composite dielectric approach. *Water Resources Research* 26, (10) (OCT): 2267-73.

Rubin, Yoram, and Susan S. (Susan Sharpless) Hubbard. 2005. *Hydrogeophysics*. Water science and technology library ; v. 5. Dordrecht, Netherlands ; New York: Springer.

Schwartz, L. M., P. N. Sen, and D. L. Johnson. 1989. Influence of rough surfaces on electrolytic conduction in porous-media. *Physical Review B* 40, (4) (AUG 1): 2450-8.

Sen, P. N., C. Scala, and M. H. Cohen. 1981. A self-similar model for sedimentary-rocks with application to the dielectric-constant of fused glass-beads. *Geophysics* 46, (5): 781-95.

Telford, William Murray, L. P. Geldart, and Robert E. Sheriff. 1990. *Applied geophysics*. 2nd ed. - ed. Cambridge [England]: Cambridge University Press.

Topp, G. C., J. L. Davis, and A. P. Annan. 1980. Electromagnetic determination of soil water content: Measurements in coaxial transmission lines. *WATER RESOURCES RESEARCH* 16, (3): 574-582.

Topp, G. C., and P. A. Ferre. 2002. The soil solution phase. In *Method of soil analysis.*, 433.

Ward, S.H. and Fraser D.C. 1967. Conduction of electricity in rocks. In *Mining geophysics.* Vol. 2, 198-223. Tulsa, OK: Society of Exploration Geophysicists.

Weitz, A. M., W. T. Grauel, M. Keller, and E. Veldkamp. 1997. Calibration of time domain reflectometry technique using undisturbed soil samples from humid tropical soils of volcanic origin. *Water Resources Research* 33, (6) (JUN): 1241-9.

Winsauer, W. O., H. M. Shearin, P. H. Masson, and M. Williams. 1952. Resistivity of brine-saturated sands in relation to pore geometry. *Aapg Bulletin-American Association of Petroleum Geologists* 36, (2): 253-77.

Appendix A

Calibration of Electrode Spacing for Wenner Array

To calibrate the spacing, the column was filled with tap water and resistivity measurements were taken using Wenner array. Syscal system applies a source of current (*I*) to the soil through electrodes, measures potential (*V*), and calculate apparent resistivity (ρ_a)

$$\rho_a = k\frac{V}{I}$$

ρ_a: apparent resistivity

k: geometric factor

V: potential

I: current

From the measurements, we have *V*, and *I* values; ρ_a was measured by a conductivity-meter, so *k* can be calculated as:

$$\rho_a = k\frac{V}{I} \rightarrow 11.87 = k\frac{352.4}{5.55} \rightarrow k = 0.187$$

Geometric factor for Wenner array at a surface of a half space is calculated as:

$$k = 2\pi a$$

where *a* is the electrode spacing. Therefore the geometric factor for the electrode spacing of 0.03 m must be:

$$k = 2\pi a = 2\pi \times 0.03 = 0.188$$

Appendix B

The basic data in Microsoft Excel (.xlsx) files and pictures of the column in .jpeg files are included on the attached CD-ROM.

Appendix C

Feenestra method

The total soil chemical concentration (Ct) is calculated as:

$$C_t = \frac{K_d C_w \rho_b + C_w \phi_w + C_w H_c \phi_a}{\rho_b}$$

where C_w is the chemical concentration in pore water (mg/L), ϕ_w and ϕ_a are the water-filled and air-filled porosity respectively, K_d is the partition coefficient between pore water and soil solids (cm^3/g), H_c is the dimensionless Henry's law constant, and ρ_b is the bulk dry density of the soil sample (g/cm^3).

Since the soil samples were analyzed for total petroleum hydrocarbon and we did not have the amount of each compound, we assumed that ethylbenzene could be representative of the API 91-01 gasoline. To find C_t of ethylbenzene in the unsaturated zone, it was necessary to know the air-filled and water-filled porosity; therefore, the water content results obtained using TDR method was used to determine the air-filled porosity in the unsaturated zone, and then the maximum ethylbenzene concentration was calculated for each point. For Borden sand and the gasoline used in this experiment, the maximum ethylbenzene that could be accounted for with a NAPL phase being present in the saturated zone is 2.3 µg/g of the dry soil, which began to decrease at the beginning of the transition zone and reached to 1.5 µg/g in the residual saturation zone. Since ethylbenzene constitutes 3.37 wt% of the API 91-01 gasoline, the maximum total amount of gasoline is about 70 µg/g in the saturated zone and then decreases gradually in the unsaturated zone until reaches to about 46 µg/g in the residual saturation zone. C_w can be calculated as:

$$C_w = S_e^i = X_i \, S_i$$

S_i: effective solubility of phase i

X_i: mole fraction of the compound i in the NAPL mixture

S_i: pure phase solubility of compound i

Ethylbenzene in API 91-01 gasoline:

C_w= 0.03(161) = 4.83 mg/L

H_c for ethylbenzene: 0.344

ρ_b of Borden sand: 1.81

Appendix D

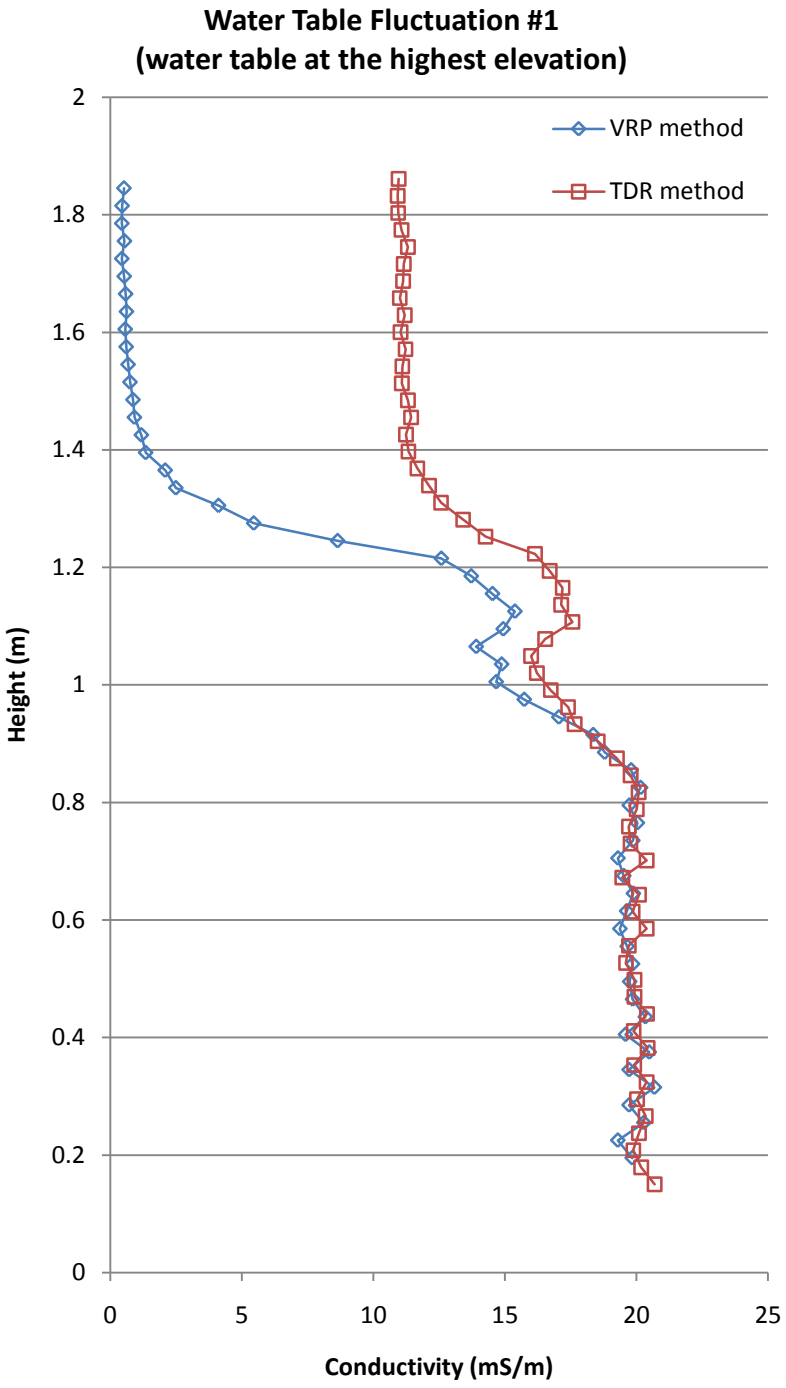
Water Table Fluctuation #1
(water table at the highest elevation)
VRP method
TDR method
Height (m)
Conductivity (mS/m)
0
0.2
0.4
0.6
0.8
1
1.2
1.4
1.6
1.8
2
0
5
10
15
20
25

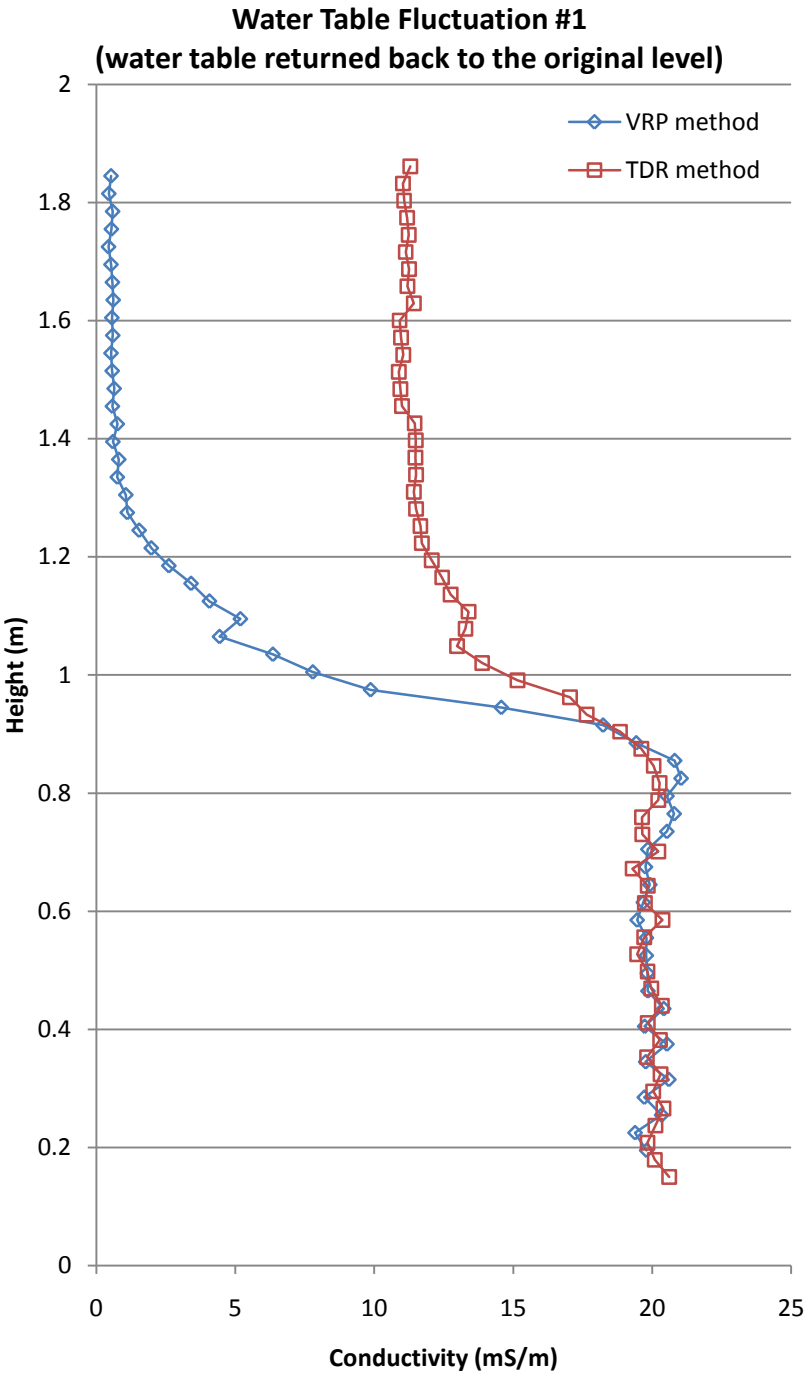
Water Table Fluctuation #1
(water table returned back to the original level)
VRP method
TDR method
Height (m)
Conductivity (mS/m)
0
0.2
0.4
0.6
0.8
1
1.2
1.4
1.6
1.8
2
0
5
10
15
20
25

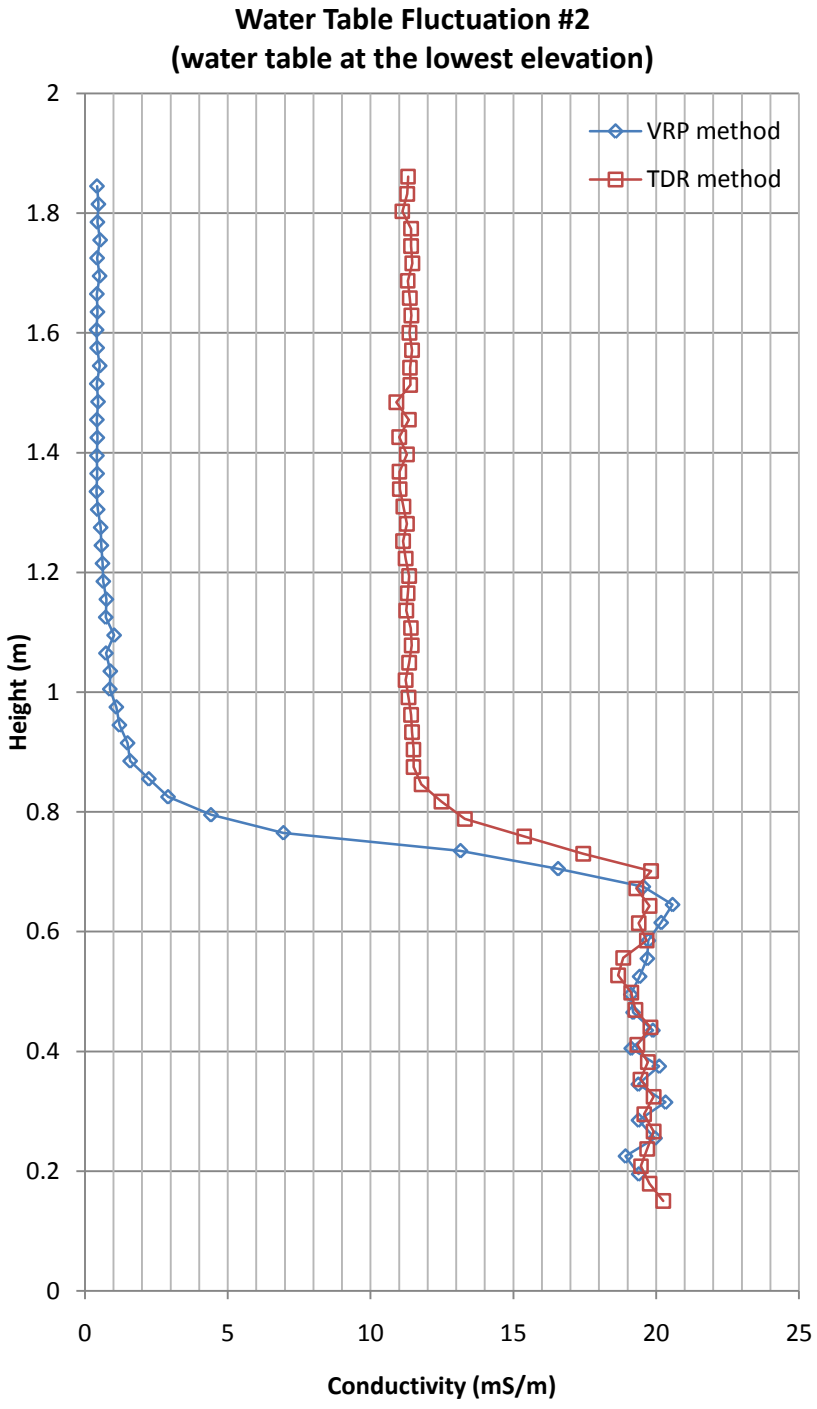
Water Table Fluctuation #2
(water table at the lowest elevation)
VRP method
TDR method
Height (m)
Conductivity (mS/m)
0
0.2
0.4
0.6
0.8
1
1.2
1.4
1.6
1.8
2
0
5
10
15
20
25

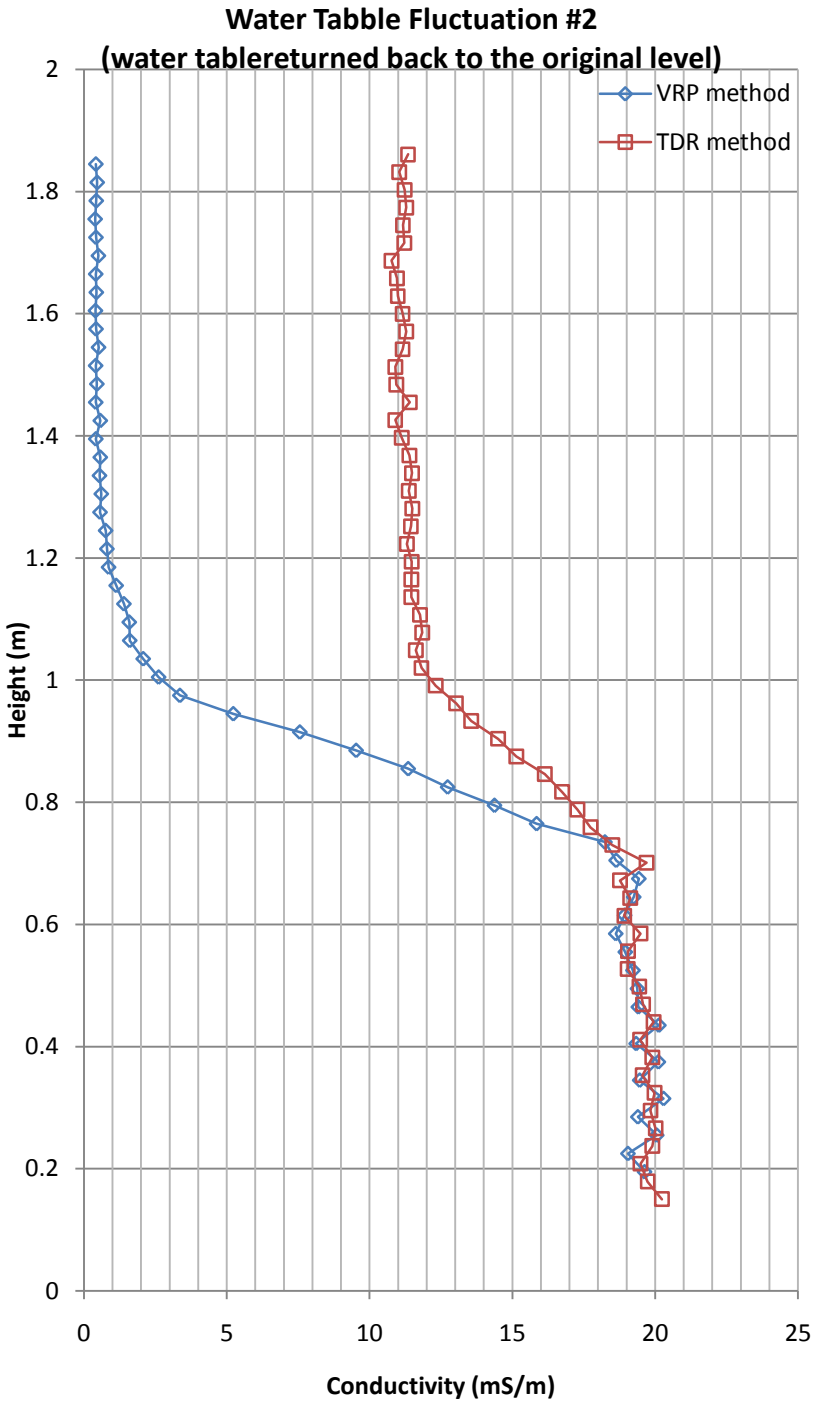
Water Tabble Fluctuation #2
(water tablereturned back to the original level)
VRP method
TDR method
Height (m)
Conductivity (mS/m)
0
0.2
0.4
0.6
0.8
1
1.2
1.4
1.6
1.8
2
0
5
10
15
20
25

Appendix E

As mentioned in section 2.1.1, Topp et al. (1980) performed a series of 18 experiments on different soil types and glass beads of different sizes with known water content and found a relationship between water content and dielectric permittivity:

$$\kappa_a = A + B\theta + C\theta^2 - D\theta^3$$

where κ_a is the apparent dielectric permittivity, θ is the volumetric water content, and A, B , C, and D are coefficients.

They classified the investigated materials into 6 groups and specified coefficients A, B, C, and D for each group. Since we usually measure κ and need to determine θ, it is necessary to have the inverse equation. In their study, Topp et al. provided the inverse relationship for all mineral soils. The inverse relationships for glass beads were found using MATLAB®. Figures 1, 2, and 3 show the original and inverse relationships for the glass beads of 30 µm, 450 µm, and a 30 µm-450 µm mixture, respectively.

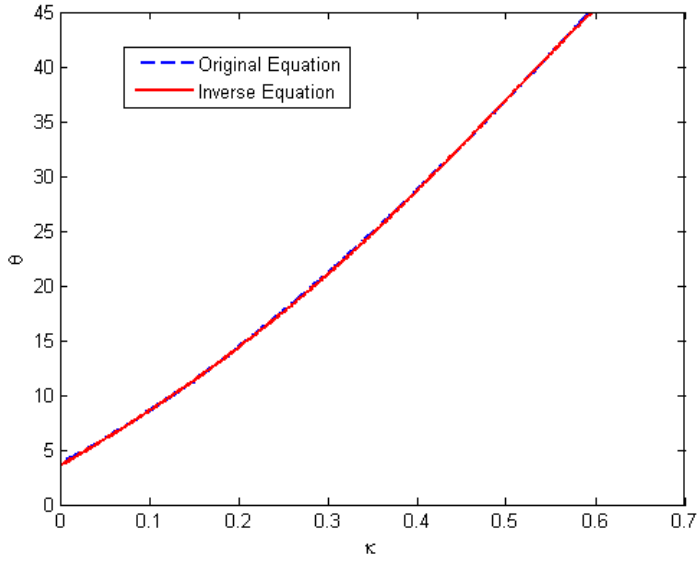

Figure 1 Glass, 30 µm: Original equation: $\kappa = 3.79 + 41.3\theta + 63.4\theta^2 - 27\theta^3$; inverse equation: $\theta = -7.96\times10^{-2} + 2.33\times10^{-2}\kappa - 3.11\times10^{-4}\kappa^2 + 2.81\times10^{-6}\kappa^3$

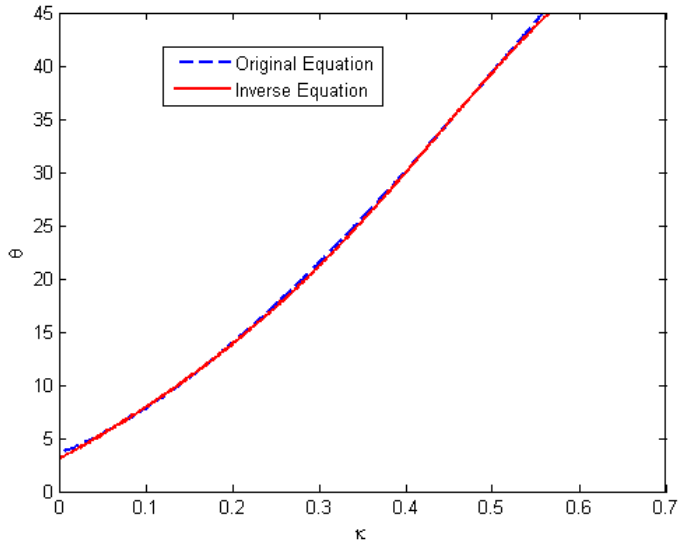

Figure 2 Glass, 450 µm: Original equation: $\kappa = 3.57 + 31.7\theta + 114\theta^2 - 68.2\theta^3$; inverse equation: $\theta = -7.17\times10^{-2} + 2.46\times10^{-2}\kappa - 4.26\times10^{-4}\kappa^2 + 4.3\times10^{-6}\kappa^3$

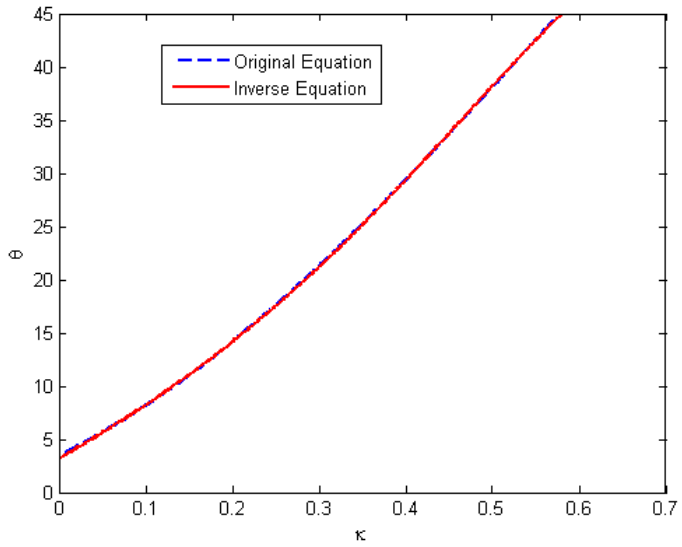

Figure 3 Glass, 30 µm and 450 µm: Original equation: $\kappa = 3.55 + 38\theta + 84.1\theta^2 - 44.1\theta^3$; inverse equation: $\theta = -7.26\times10^{-2} + 2.35\times10^{-2}\kappa - 3.53\times10^{-4}\kappa^2 + 3.39\times10^{-6}\kappa^3$